



**UNIVERSITÀ
DEGLI STUDI
DI PADOVA**

Sede Amministrativa: Università degli Studi di Padova

Dipartimento di Biologia

SCUOLA DI DOTTORATO DI RICERCA IN BIOSCIENZE E BIOTECNOLOGIE
INDIRIZZO DI BIOLOGIA CELLULARE
CICLO XXV

**Impact of *S.pneumoniae* type-I pilus and its subunits on bacterial
adherence to human epithelial cells**

Direttore della Scuola: Ch.mo Prof. Giuseppe Zanotti

Coordinatore d'indirizzo: Ch.mo Prof. Paolo Bernardi

Supervisore: Ch.mo Prof. Cesare Montecucco

Co-supervisore: Dott. Alfredo Pezzicoli

Dottoranda: Fulvia Amerighi

Index

INTRODUCTION	- 3 -
PATHOGENESIS OF PNEUMOCOCCAL DISEASE: COLONIZATION AND INVASION	- 4 -
EPIDEMIOLOGY.....	- 6 -
PNEUMOCOCCAL VACCINE	- 7 -
PILI IN GRAM POSITIVE AND NEGATIVE BACTERIA	- 9 -
PILI IN <i>S.PNEUMONIAE</i>	- 12 -
<i>Pilus1 and pilus2</i>	- 12 -
<i>Crystal structure of RrgA and RrgB proteins</i>	- 16 -
<i>Biphasic expression pattern of pilus1</i>	- 17 -
<i>Role of S.pneumoniae pilus1</i>	- 18 -
MATERIAL & METHODS	- 20 -
BACTERIA STRAINS AND GROWTH CONDITIONS.....	- 21 -
CELL CULTURE TECHNIQUES.....	- 21 -
ADHESION ASSAY	- 22 -
ADHESION INHIBITION ASSAY.....	- 22 -
CONFOCAL IMMUNOFLUORESCENCE MICROSCOPY	- 22 -
IMMUNOGOLD LABELING AND ELECTRON MICROSCOPY	- 23 -
GENOMIC DNA EXTRACTION	- 24 -
CONSTRUCTION OF 19F TAIWAN14 CAPSULAR DELETION MUTANT.....	- 24 -
POLYMERASE CHAIN REACTION (PCR).....	- 25 -
STREPTOCOCCUS PNEUMONIAE TRANSFORMATION.....	- 26 -
COLONY IMMUNO-BLOT	- 26 -
WESTERN BLOT ANALYSIS	- 26 -
FLOW CYTOMETRY ANALYSIS	- 27 -
EPI TOPE MAPPING.....	- 27 -
RESULTS	- 29 -
INVOLVEMENT OF PNEUMOCOCCAL TIGR4 STRAIN PILI IN THE ADHESION TO DIFFERENT EPITHELIAL CELLS	- 30 -
<i>Adhesion to ME180</i>	- 30 -
<i>Adhesion to A549, MDCKII and Calu-3</i>	- 31 -
CONFOCAL MICROSCOPIC ANALYSIS AND ELECTRON MICROSCOPY STUDIES USING ME180 CELL LINE CONFIRMS THE CONTRIBUTION OF PILUS COMPONENTS TO PNEUMOCOCCAL ADHESION TO EPITHELIAL CELLS	- 33 -
TYPE I PILUS MEDIATED ADHESION TO CELLS VARIES AMONG DIFFERENT <i>S.PNEUMONIAE</i> STRAINS.....	- 38 -
PILUS DEPENDENT ADHESION TO HOST CELLS IS MODULATED BY CAPSULE THICKNESS	- 39 -
ANTIBODIES AGAINST PILUS COMPONENTS REDUCE THE CAPACITY OF PILIATED BACTERIA TO ADHERE TO THE EPITHELIAL MONOLAYER	- 42 -
FACS ANALYSIS SHOWS THAT ANTI-RRGA MABS BINDING TO T4 H CORRELATES WITH INHIBITION OF ADHESION	- 44 -
EPI TOPE MAPPING STUDIES IDENTIFY A VARIABLE LOOP IN DOMAIN 3 OF RRG A AS THE PUTATIVE TARGET FOR MAb 11B9/61.....	- 45 -
DISCUSSION AND CONCLUSIONS	- 49 -

Introduction

Pathogenesis of pneumococcal disease: colonization and invasion

Streptococcus pneumoniae (figure 1) is a lancet-shaped gram-positive bacterium which is present in the normal bacterial flora of the human upper respiratory tract together with other commensal microorganisms like *Moraxella cattarrhalis*, *Haemophilus influenzae*, *Neisseria meningitidis* and *Staphylococcus aureus*. Even though pneumococcal colonization is mostly symptomless, it can occasionally lead to severe respiratory infections such as acute otitis media, sinusitis and pneumonia (Fletcher and Fritzell, 2007; O'Brien et al., 2009; Ryan and Antonelli, 2000).

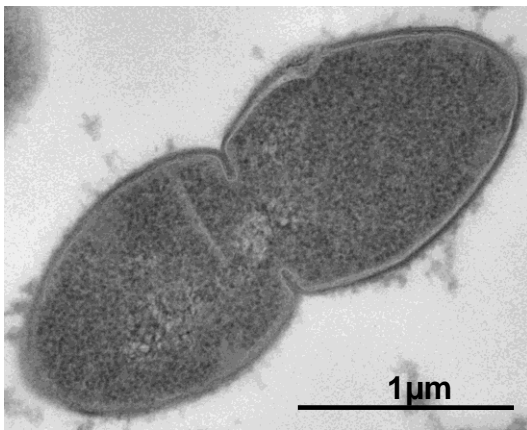


Fig. 1 Electron microscopy image of *Streptococcus pneumoniae* TIGR4 strain.

Indeed *S.pneumoniae* is capable of translocating from the nasopharynx to the lung, where it causes pneumonia, or it can migrate directly to the blood, giving rise to bacteremia, septicemia and eventually meningitis (Bogaert et al., 2004a).

Pneumococcal colonization is commonly followed by the horizontal dissemination of the bacterium among individuals of a shared environment, leading to the rapid diffusion within the community (Givon-Lavi et al., 2002). The reported rates of bacterial acquisition and carriage depend on age, geographical area, genetic background, and socioeconomic conditions, suggesting that young children, elderly people and patients with immunodeficiencies are the groups with higher probability to develop pneumococcal driven diseases (ACIP, 1997).

S. pneumoniae colonization is a dynamic process that depends on various factors among which the level of nasopharyngeal colonization by commensal microorganisms and the host immune response are the most important. Indeed the bacterium competes with the resident

flora which has its primary role in inhibiting the attachment and colonization of pathogens. On the other hand a poor mucosal immune response might lead to persistent and recurrent colonization and consequently infection, whereas a brisk local immune response to the pathogen will eliminate colonization and prevent re-colonization. Nasopharyngeal colonization is the initial step from which mucosal and invasive pneumococcal infection develops (Fig. 2).

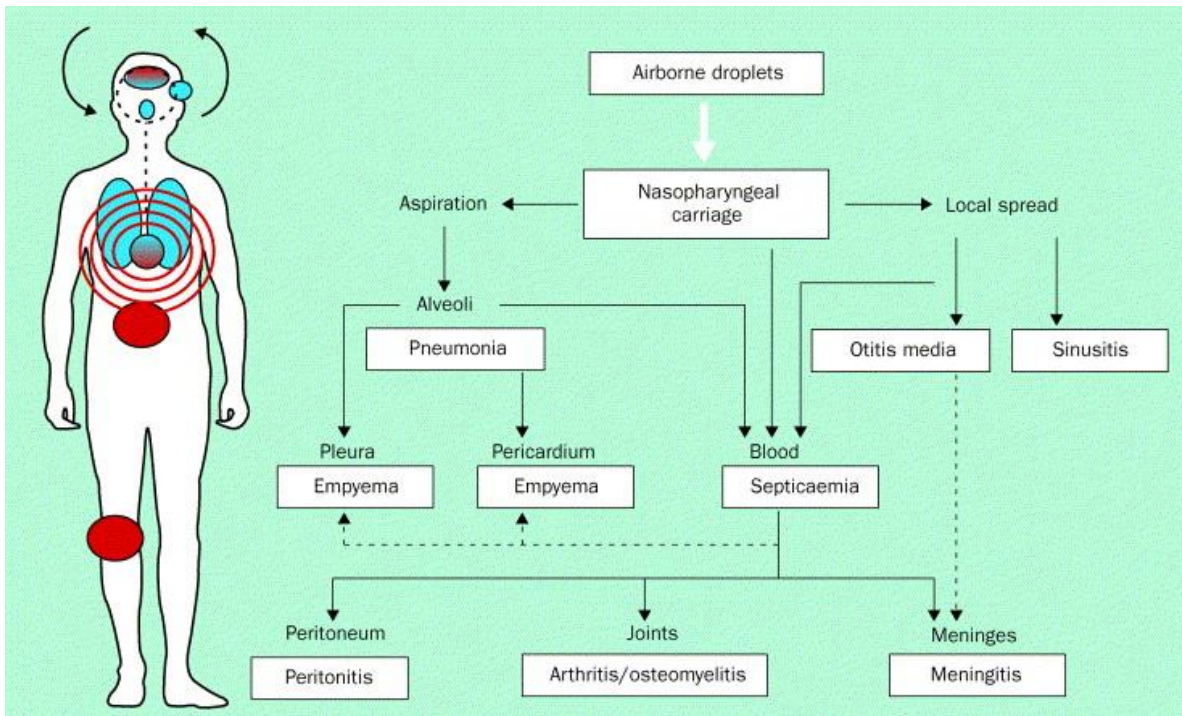


Fig. 2 Pathogenic route for *S. pneumoniae* infection. Organs infected through the airborne and haematogenic routes are showed in blue and red, respectively (Image from Bogaert et al., 2004b).

Many antibiotics such as fluoroquinolones, doxycyclin, and trimethoprim-sulfamethoxazole have been used for the treatment of pneumococcal infections. However, the development of antibiotic resistance has become a worldwide problem and thus pneumococcus remains a major cause of morbidity and mortality. For this reason great efforts are being made to develop effective vaccines for the prevention of the pneumococcal diseases. *S.pneumoniae* produces a panel of colonization and virulence factors, including the polysaccharide capsule, surface proteins and enzymes, and the pneumolysin toxin, that allow the bacterium to escape the host immune system and cause disease.

The polysaccharide capsule is probably the most important virulence factor in pneumococcal disease, mainly because it is able to protect bacteria from immuno-mediated phagocytosis (Henrichsen et al., 1995). Indeed the capsule surrounds the bacterial cell blocking the access of antibodies and complement factors to the pneumococcal surface, leading to an impaired immune system clearance. On the other side capsular polysaccharides are highly immunogenic and antibodies targeting pneumococcal polysaccharides are able to protect against infections caused by homologous serotypes by inducing opsonophagocytic mechanisms (Kadioglu et al., 2008).

Epidemiology

More than 90 serotypes have been identified based on the antigenic profile of the polysaccharide capsule. Some of these serotypes exhibit a distinctive epidemiology with regard to their potential to cause invasive disease, their occurrence in specific age groups or geographic regions, their association with antibiotic resistance and their epidemic potential (Hausdorff et al., 2005). Most *S. pneumoniae* serotypes have been shown able to cause serious diseases, but, in each region, only few serotypes (and mainly region specific) account for the majority of pneumococcal infections, with serotype composition changing upon seasonal and epidemic variations due to different clones spread. Serotypes 1, 5, 6, 7, 14, 18, 19, and 23 are the most prevalent worldwide, accounting for 60-80% of the invasive diseases, depending on the area of the world. The serotype distribution among nasopharyngeal carriage isolates varies slightly by country, age-group, and type of cohort. Although capsular serotyping is currently the most widely used and efficacious strategy for classification of pneumococcal strains, this method presents some limitations like the inability to quantify the genetic relationship between isolates. In order to overcome these limitations, a nucleotide sequence based method, Multi Locus Sequence Typing (MLST), has been developed in the last decade. This method involves the sequencing of internal fragments from seven house-keeping genes, and the unequivocal assignment of the isolates to a sequence type (ST) (Chan et al., 2001). Moreover, through the algorithm eBURST single STs can be grouped in Clonal Complexes (CCs) based on the number of differences in their allelic profile (Spratt et al., 2004; Feil et al., 2004), and sequence data can be held on a central database (<http://www.mlst.net>) and queried through a web server. Interestingly, there is no univocal correspondence between the two classification methods, therefore, in defining an isolates both

serotyping and MLST typing are needed, as serotypes are usually associated to more than an ST type and vice-versa (Chan et al., 2001).

Pneumococcal vaccine

Despite *S. pneumoniae* pathogenic mechanisms, host-pathogen interactions and the bacterial disease determinants have been studied for over a century, invasive pneumococcal disease kills over 1.5 million children each year (<http://www.who.int/vaccines/en/pneumococcus.shtml>). Antibiotic therapy still remains efficacious for *S. pneumoniae* disease treatment, but, due to the increasing antibiotics resistance, vaccination represents the most effective strategy for preventing pneumococcal infections. Although different serotype-based vaccines are already present on the market, their use presents some limitations. The 23-valent polysaccharide based vaccine (Pneumovax 23®, marketed by Merck & Company, Inc.) contains 23 different capsular polysaccharides (1, 2, 3, 4, 5, 6B, 7F, 8, 9N, 9V, 10A, 11A, 12F, 14, 15B, 17F, 18C, 19A, 19F, 20, 22F, 23F, and 33F) (Cadoz et al., 1985). This vaccine is not effective in children under 2 years of age and immunocompromised patients (ACIP). Moreover vaccination with Pneumovax 23® resulted effective only against bacteremia and meningitis in the elderly population, but not against pneumonia, the most prevalent pneumococcal disease of this age group (Mangtani et al., 2003; Jackson et al., 2003).

Other vaccines present on the market include: the 7-valent (PCV-7 or Prevnar) targeting seven serotypes (4, 6B, 9V, 14, 18C, 19F and 23F), the 10-valent (Synflorix™) covering serotypes 1, 4, 5, 6B, 7F, 9V, 14, 18C, 19F and 23F conjugated to *Haemophilus influenzae* protein-D (PHiD-10), and the 13-valent conjugate vaccine covering serotypes 1, 3, 4, 5, 6A, 6B, 7F, 9V, 14, 18C, 19A, 19F and 23F (PCV-13 or Prevnar-13). These vaccines are effective on the target populations, but their strain coverage is serotype-dependent and can favor serotype replacement (Bogaeret et al., 2004a; Cauchemez et al., 2006; Toltizis et al., 2005).

In addition the prohibitive costs of producing conjugate vaccines are a limit for their use in developing countries with the highest burden of disease and poor economical resources. For these reasons, vaccine research is currently focusing toward the use of potential vaccine components consisting of one or more universally conserved protein antigens, able to elicit serotype-independent protection (Ryan et al., 2000, Toumanen et al., 1999). Pneumococcal surface-exposed proteins have attracted considerable attention as a consequence of their potential use as vaccine antigens, able to stimulate the production of opsonic antibodies.

Three major groups of pneumococcal cell-surface proteins have been identified so far: choline-binding proteins (Cbps), lipoproteins and proteins that are covalently linked to the bacterial cell wall by a carboxy C-terminal sortase motif (LPXTG: in which X denotes any amino acid) (Fig 3).

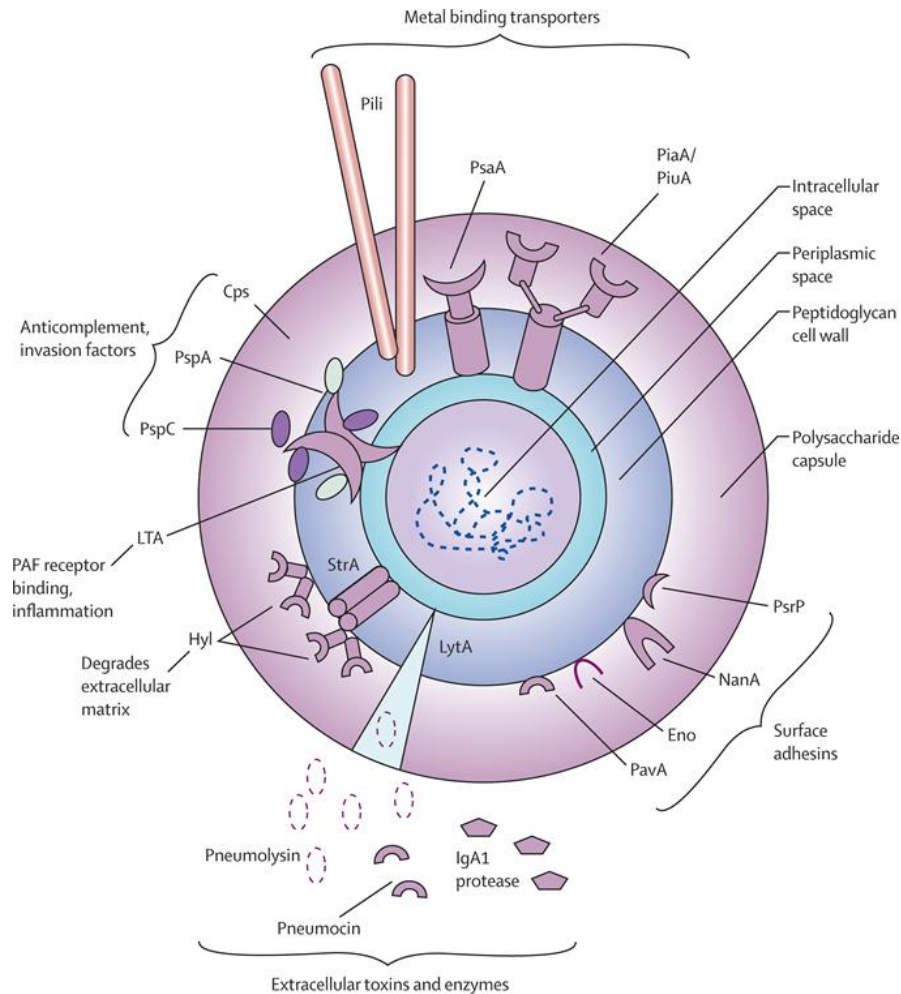


Fig. 3 Schematic representation of pneumococcal virulence factors (Image from van der Poll T et al., 2009).

Up to now *S. pneumoniae* results as the sole human pathogenic bacterium known to express proteins that are associated to the bacterial surface by binding choline residues present in the cell-wall peptidoglycan. Interestingly, all the three known pneumococcal autolysins (LytA, LytB and LytC) and PspA belong to this category, and several Cbps, like CbpA, CbpD, CbpE and CbpG are bacterial factors implicated in colonization processes (Berry et al.1989). In

addition to the already known factors differently implicated in bacterial pathogenesis, the recent discovery that gram-positive pathogens express pili (Telford et al., 2006; Ton-That et al., 2004), has opened a new area of research into their function in pathogenesis and their role as protective antigens.

Pili in gram positive and negative bacteria

The surface components of a pathogenic bacterium are usually involved in the interaction of the microorganism with the environment where it lives and hence they often are major virulence factors. Pili and fimbriae are long filamentous appendices that are presented by Gram-positive and Gram-negative bacteria on their surface. These structures play a key role in host cell adhesion and invasion, biofilm formation, cell aggregation and DNA transfer as it has been reported by different studies (Proft and Baker, 2009).

For numerous bacterial pathogens pili-like structures are reported to be virulence factors and various studies designate them as eligible components for vaccine development (Gianfaldoni et al, 2007; Maione et al, 2005; Margarit et al, 2009; Mora et al, 2005; Proft & Baker, 2009). The role of pili as adhesive organelles is of particular importance for pathogenic bacteria as they are involved in the attachment to specific host ligands during colonization of host niches. In particular it has been proposed that bacteria use these structures to form an initial association with host cells, which can then be followed by a more “intimate” attachment that brings the bacterium into close proximity to the host-cell surface. Pili of Gram negative bacteria are known to adhere to components of the extracellular matrix (ECM), are variable in thickness (from 2 up to 7nm) and are composed by non-covalent homo-polymerized major subunits.

Gram-positive bacteria use the cell wall as a scaffold for displaying a wide variety of surface molecules that may be either non-covalently attached to the cell wall or covalently linked to the peptidoglycan. Among the latter are pilus-like structures, long and flexible appendages with a diameter ranging from 3 to 10 nm and composed by covalently linked major subunits (backbone pilus proteins) and ancillary subunits that are assembled together by specialized sortase enzymes (Telford et al., 2006). By the use of electron microscopy, pilus-like structures have been identified for the first time in the Gram-positive bacterium *Corynebacterium renale* (Yanagawa et al., 1968). These structures were also reported in many other species such as *Actinomyces naeslundii*, *Corynebacterium diphtheriae*, and many oral *Streptococcus spp* (Thon That H. & Schneewind O. 2004a; Telford et al., 2006). Gram-positive pili are usually

encoded by islets inserted into specific genomic regions, varying in length and genetic organization, but sharing characteristic features; all pilus encoding islets contain genes coding for LPXTG or LPXTG-like surface-anchored proteins that are the pilus major and minor components and for sortase enzymes, specialized transpeptidases involved in pilus assembly. The first insights into the assembly mechanism of Gram-positive pili were provided by Ton-That and Schneewind on *Corynebacterium diphtheriae* (Ton-That and Schneewind, 2003). They showed that various conserved genetic elements present within the major pilin subunit are required for a correct sortase-mediated pilus assembly: the pilin motif (WxxxVxVYPK) providing the ϵ -amino group in the lysine (K) residue is required for subunit polymerization; the E-box domain (YxLxETxAPxGY) and a C-terminal cell wall sorting signal (LPxTG or a variant thereof), followed by an hydrophobic domain and a positively charged tail (Ton-That & Schneewind, 2003; Ton-That & Schneewind, 2004a; Ton-That et al. 2004b) (Figure 4).

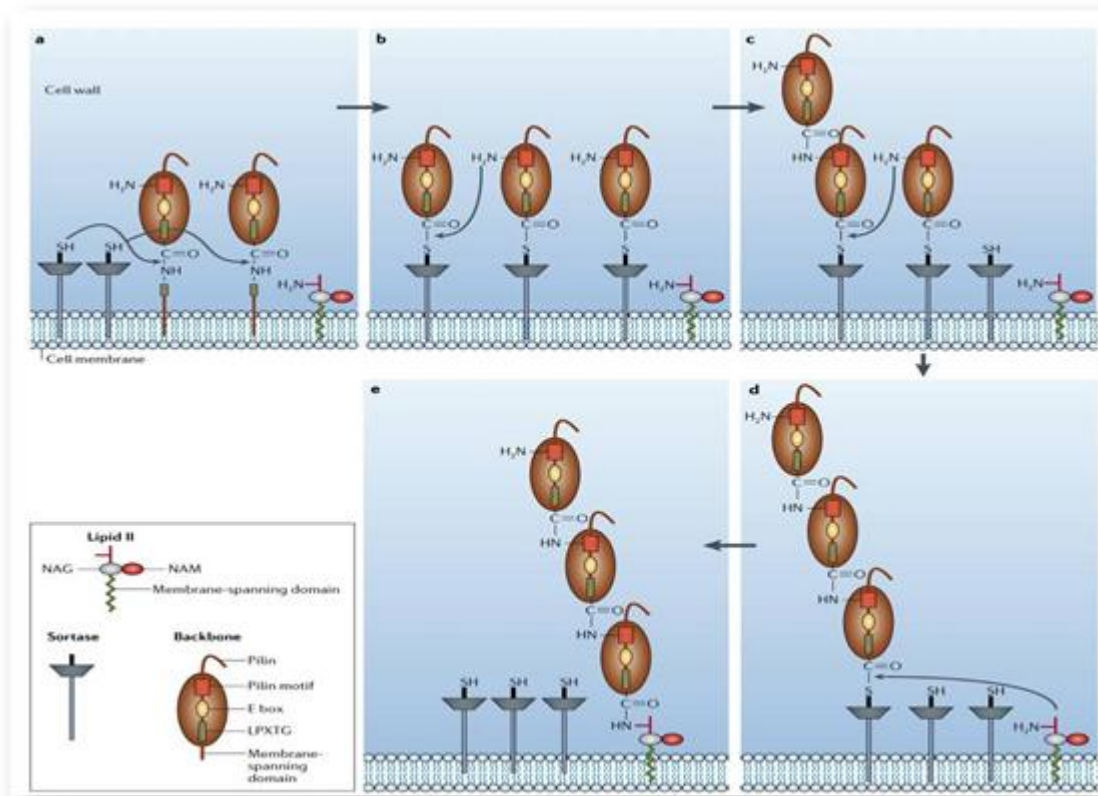


Fig. 4 Model of pilus assembly. A) In the first step, proteins that contain the LPXTG motif (where X denotes any amino acid) are targeted to the cell membrane by Sec-dependent secretion (not shown). Afterwards the LPXTG motif is cleaved between the threonine (T) and glycine (G) residues (indicated by the arrows). B) The reaction leads to the formation of an acyl-enzyme intermediate in which a covalent thioester bond is formed between the thiol group of a cysteine residue in the sortase and the carboxyl group of the pilin threonine residue. C) Oligomerization occurs through the nucleophilic

attack by the ϵ -amino group of the lysine residue in the pilin motif on the thioester bond of the sortase intermediate. D) As a final point, the thioester bond between the pilin subunit and the sortase is targeted by the amino group of the pentapeptide of lipid II, the precursor of peptidoglycan. E) This leads to the formation of a membrane-associated, covalently linked, elongated pilus. NAG, N-acetyl glucosamine; NAM, N-acetyl muramic acid. (Image from J. Telford et al. 2006).

Following this observation, several other investigations were performed in different pilus-expressing streptococci (*S. pneumoniae*, *S. pyogenes* and *S. agalactiae*) (Mora et al., 2005; Lauer et al., 2005; Barocchi et al., 2006). Taken together, mutant studies, biochemical data and the recently solved crystal structure of the *Streptococcus pyogenes* pilus backbone (Kang et al., 2007), which elucidated the peptidyl linkage of one major pilin subunit to the next, lend support to the “sortase-mediated pilus assembly” mechanism proposed by Ton That and Schneewind as a general model for pilus assembly in Gram-positive bacteria (Ton-That & Schneewind 2003).

According to this hypothesis, the LPXTG or LPXTG-like motif, is the target of the sortases (membrane anchored transpeptidases usually coded by genes present in the pilus islets and different from the housekeeping sortase enzyme SrtA), which during pilus formation catalyse the covalent attachment of the subunits (pilins) to each other and to the peptidoglycan cell wall. In detail, the sortases connect consecutive backbone pilins through covalent inter-molecular isopeptide bonds linking the threonine residue of the LPxTG motif and the ϵ -amino group of the lysine residue located in the pilin motif at the N-terminus of the next subunit. Interestingly, the pilin motif is not a universal feature for all pilus components; most *S. pyogenes* (GAS) pilins do not harbor a classical pilin motif, and in this case other lysines were experimentally identified as implicated in the formation of the inter-molecular isopeptide bonds (Kang et al., 2007) suggesting that multiple different sites can be targeted by sortases to polymerize pili on the bacterial surface. In addition, one or more accessory subunits (minor pilins) are incorporated into the pilus, along the structure or at the boundaries, by a similar mechanism requiring one or more sortases, as well as the conserved E-box domain within the major pilin protein.

Interestingly, Kang et al. observed for the first time the presence of intra-molecular isopeptide bonds within the *S. pyogenes* backbone pilin and suggested a possible role for these bonds in stabilizing the overall structure of the pilus components as well as of the single domains. In general, this structural organization appears to be a peculiar characteristic of Gram-positive

bacteria since to date no intra or inter molecular covalent bonds have been described in Gram-negative bacteria pili (Kang et al. 2007; Budzik et al., 2008).

Pili in *S.pneumoniae*

Pilus1 and pilus2

By *in silico* analysis of *Streptococcus pneumoniae* genomes, two genomic elements containing genes distinctive of Gram-positive pili have been identified, the pilus islet 1 (PI-1) and the pilus islet 2 (PI-2) (Barocchi et al., 2006 ; Bagnoli et al., 2008) (Figure 5).

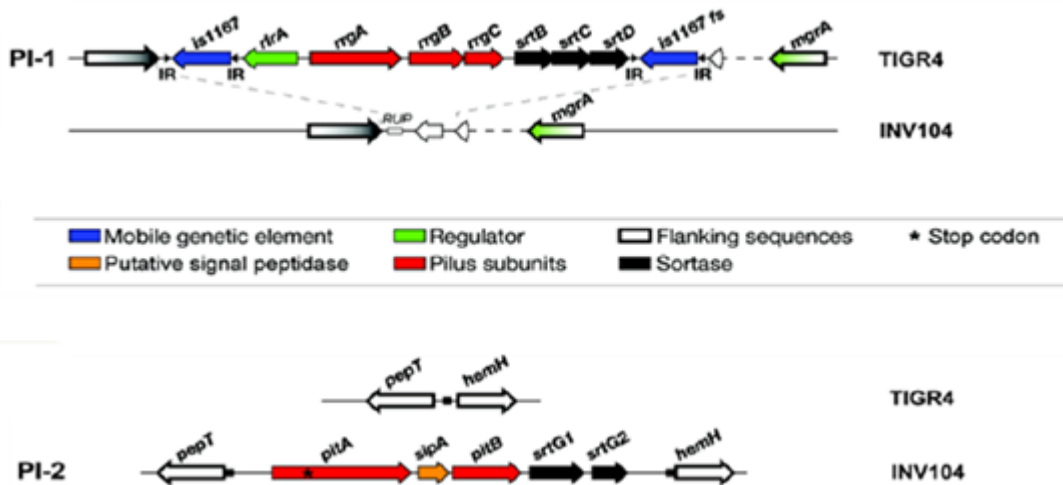


Fig. 5 Genomic organization of pilus-encoding islets in *S. pneumoniae*. Schematic representation of PI-1 and PI-2 (Image from Bagnoli et al; 2008).

The presence of both these genetic islets results in the functional polymerization of pilus-like structures on the surface of pneumococcal bacteria even though not all isolates carry one of the two islets in their genomes. Indeed, molecular epidemiology and genomic analyses demonstrated that, differently from *S.pneumoniae*, all *S.pyogenes* and *S.agalactiae* isolates code for at least one functional pilus, suggesting possible different roles for pili in the disease outcome of these major streptococcal pathogens (Basset et al., 2007; Moschioni et al., 2008; Margarit et al., 2009; Falugi et al., 2008). In detail, PI-1, firstly identified in the genome of the TIGR4 strain, is a chromosomal region of approximately 12 kb, flanked by two insertion

sequences (IS1167) and comprising seven genes: *rlrA*, encoding a RofA-like transcriptional regulator which positively regulates pilus expression (Hava et al., 2003) and its own expression, *rrgA*, *rrgB* and *rrgC*, which encode the LPxTG cell-wall anchored pilin subunits, and *srtC-1*, *srtC-2* and *srtC-3* coding for the three sortases involved in the linkage and assembly of the pilus structure on the bacterial surface (LeMieux et al., 2006 ; LeMieux et al., 2008; Falker et al., 2008; Manzano et al., 2008). Recently it has been demonstrated that RrgB is the major subunit that forms the backbone of the structure, RrgA is the major ancillary protein, localized at the pilus tip and responsible for the adhesion, whereas RrgC is the minor ancillary protein, likely located at the pilus base and responsible for the putative cell wall anchoring (Hilleringmann et al., 2009; Hilleringmann et al., 2008, Nelson et al., 2007) (Figure 6).

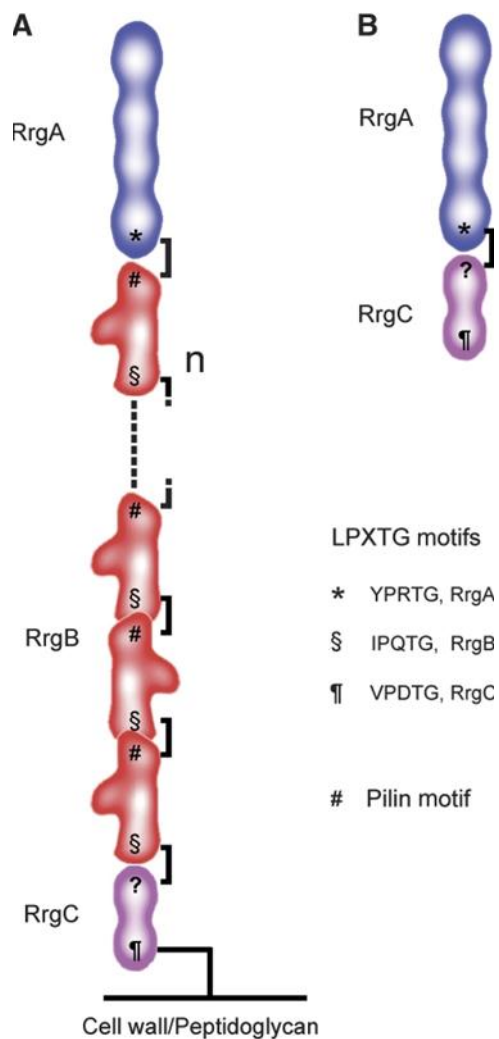


Fig. 6 Model of *S. pneumoniae* pilus1. (A) TIGR4 pilus1 is a flexible filament formed by repetitive RrgB monomers decorated with two ancillary proteins: RrgA and RrgC located at the tip and base of the shaft respectively. Sortase SrtC-1 mediates the polymerization of RrgB via the LPXTG motif (*,

IPQTG) and pilin motif (#), covalently linked head-to-tail. C-type sortases also control the addition of the ancillary proteins and anchor RrgC to the peptidoglycan cell wall, depending on the recognition of the respective LPXTG motifs YPRTG (RrgA) and VPDTG (RrgC). (B) RrgA and RrgC show the ability to form a heterodimer suggesting a site in RrgC that can be covalently linked to an LPXTG motif from either RrgA or RrgB (Image from Hilleringmann et al., 2009).

Recent data showed that the deletion of all three pilus-associated sortase genes, *srtC-1*, *srtC-2* and *srtC-3*, completely prevented pilus biogenesis, and expression of SrtC-1 alone is sufficient to covalently associate RrgB subunits to one another as well as linking the RrgA adhesin and RrgC into the polymer (Falker et al., 2008; Lemieux et al., 2008). In particular, Falker's studies suggested that, SrtC-1 and SrtC-2 act as redundant pilus subunit polymerases, with SrtC-1 processing all three pilus subunits proteins, while SrtC-2 only RrgA and RrgB. In contrast, SrtC-3 seems to have no pilus polymerase activity, but appears to be required for wild type focal presentation of the pili on the bacterial surface. The PI-2 islet, identified by Bagnoli et al. in 2008, is a 7-kb region containing five genes coding for two putative sortases (*srtG1* and *srtG2*), a signal peptidase related protein (*sipA*) essential for pilus assembly and two LPXTG-type surface anchored proteins, *pitB* and *pitA*, where the first is the backbone subunit and the latter the ancillary protein. Interestingly, probably due to the different function of the two structures, several copies of pilus1 are present on the bacterial surface, whereas only a single copy of pilus2 is detectable for each diplococcus (Fig 7).

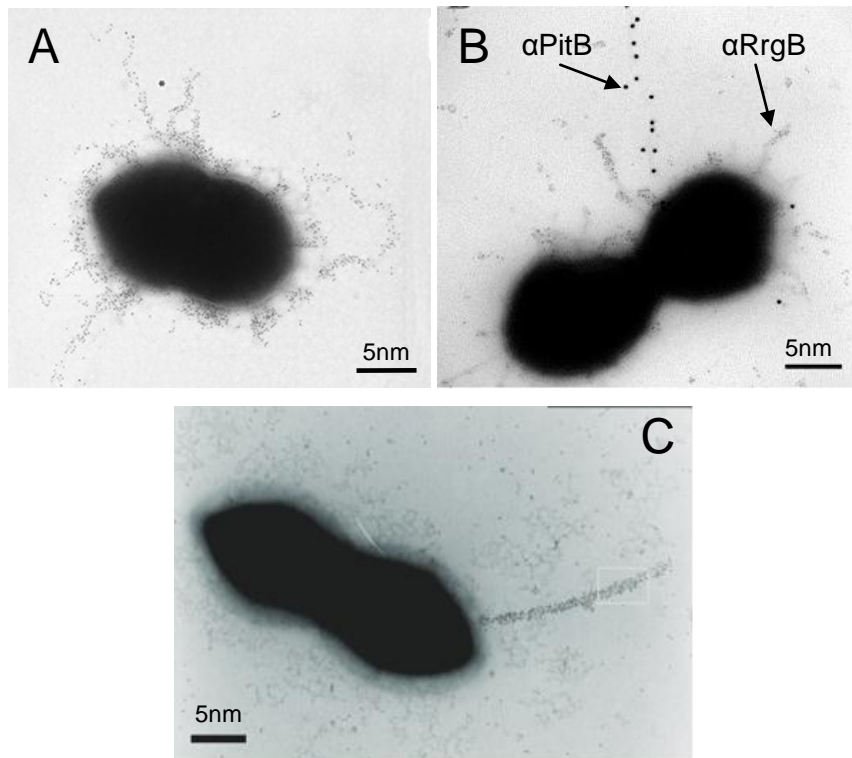


Fig. 7 Immunogold localization of: pilus1 in T4 strain with α RrgB (Image from Barocchi et al., 2006) (A); both pilus1 and pilus2 in 19FTaiwan14 strain with α PitB and α RrgB (B) and only pilus2 in PN110 strain with α PitB (C) (Images from Bagnoli et al., 2008) (secondary antibody is conjugated to 5nm gold particles).

Analysis of global *S. pneumoniae* collections revealed that in both invasive and nasopharyngeal clinical isolates the frequency of the PI-1 islet was ~30% and that the presence of PI-1 was correlated with the genotype of the isolate, as defined by multi locus sequence typing (MLST), but not with the serotype (Moschioni et al., 2008; Aguiar et al., 2008; Basset et al., 2007).

Furthermore the incidence of PI-1 was higher among antibiotic resistant clones (~50%) (Moschioni et al., 2008) thus suggesting that the pilus encoded by PI-1 may play a role in the global spread of antibiotic non-susceptible pneumococci (Sjostrom et al., 2007). A recent study demonstrated that PI-2 is present in ~16% of invasive and nasopharyngeal clinical isolates (Bagnoli et al. 2008) and that the presence of the islet is also correlated with the genotype. Interestingly both islets are present in the Taiwan19F-14 (ST236) clone, whose spread is responsible for the increasing incidence of antibiotic resistant isolates in many countries (Maiden, 1998). Extensive sequencing of PI-1 and PI-2 from different PI positive strains allowed, based on sequence similarities, the identification of three major variants of

the PI-1 operon namely clade I, II and III, while all the PI-2 isolates fell into a single clade. Interestingly, strains harboring the same genotype were also homogeneous for the PI-1 clade. More detailed studies revealed that the most variable proteins within PI-1 are the pilus components RrgB and RrgA displaying an overall homology respectively of 49%-67% and 84%-98%. The most conserved components are RrgC and the sortases (98%-99%). RrgB exist in three major clades (I, II and III), whereas RrgA is present in two variants (clade I and II). Interestingly, RrgA clade I isolates harbor RrgB clade I and III whereas RrgA clade II isolates harbor RrgB clade II (Moschioni et al. 2008).

Crystal structure of RrgA and RrgB proteins

An important step in understanding the interaction of *S.pneumoniae* pili with host targets is the recent characterization of the structures of pilus1 sub-units (Izore et al., 2010; Paterson et al., 2011). RrgA is a protein of 893-residue composed by four domains (D1, D2, D3 and D4) linked by flexible regions and harbors two intramolecular isopeptide bonds, located in D2 and D4 domain respectively (Izore et al., 2010). This architecture can hypothetically allow the flexibility of interdomain, which could be a crucial step for the recognition of different host targets, while the presence of the isopeptide bonds guarantees the stability of the individual domains. The D1 and D4 domains are highly reminiscent of an IgG domain, whereas D2 domain is reminiscent of that of the B domain of the collagen-binding adhesion Cna from *Staphylococcus aureus* (Deivanayagam et al., 2000). The D2 domain is linked to a third major domain (D3) that contains two motifs that potentially recognize components of the extracellular matrix: a von Willebrand-like factor that harbors two arms extruding from the core and a basic U-shaped cradle located between the two arms. D1, D2 and D4 domains are associated linearly with D3 placed at the edge, suggesting that one of the roles of D1, D2 and D4 domains is probably to project the D3 domain away from the protein core to allow the interaction with host cells receptors. Moreover the crystal structure of an RrgB portion, spanning from AA184 to AA627, has been solved revealing the presence of three domains, namely D2, D3, and D4. The crystal data analysis showed that domains D2 and D3 are structurally homologous to each other, both consisting of a pair of four stranded β -sheets forming a β -sandwich. The domain D4 is composed of 181 residues and, in addition to the beta strands, it contains an anti-parallel alpha helix motif. Moreover, each of the three domains of RrgB contained an intra-molecular isopeptide bond. Interestingly, sequence alignment analysis performed on different RrgB clades (I, II, and III) from different strains

and some pilus backbone sequences of other streptococci like *S. pyogenes* and *S. agalactiae* revealed that all the residues involved in the intra-molecular isopeptide bonds formation are conserved, underlining the critical role of these bonds in maintaining pilus integrity and stability. The RrgB N-terminal D1 domain structure, missing in the crystal, was then obtained by molecular modeling, by aligning and then threading the sequence of D1 onto the crystal coordinate of the N-terminal domain of *S. pyogenes* spy0128; the residues corresponding to longer gaps, were manually modeled and the resulting structure was then refined by energy minimization (Spraggon et al., 2010).

Biphasic expression pattern of pilus1

The molecular organization of pilus1 and the mechanism of pilus assembly have been largely studied and a panel of putative PI1 genetic regulators have been identified (Hilleringmann et al., 2009, Hemsley et al., 2003; Song et al., 2009, Manzano et al., 2008, LeMieux et al., 2008, Spraggon et al., 2010). Conversely little is known regarding the regulation of pilus expression as well as the environmental conditions able to modulate it. Recently it has been reported that pilus expression is not homogenous when analyzed at the single-cell level (De angelis et al, 2011). Indeed, among the same isolate, there are cells expressing pili and other that result negative for the presence of the pilus structure (biphasic expression). Indeed, by single colony isolation, it is possible to separate two distinct populations, one expressing pilus at high levels named sub-population H and the other one expressing pilus at low levels named sub-population L (Fig.8). The proportions of H and L sub-populations are variable among the strains and seem to be not influenced by serotype, genotype, growth conditions and colony morphology. Interesting the absence of genetic variations in the PI1 sequence between the two sub-populations was observed. Moreover, by comparing the transcriptional profiles of the H and L sub-populations, is evident that PI1 components expression is regulated, with on/off mechanism, at the transcriptional level. The molecular mechanism responsible for the biphasic pilus phenotype is still under investigation.

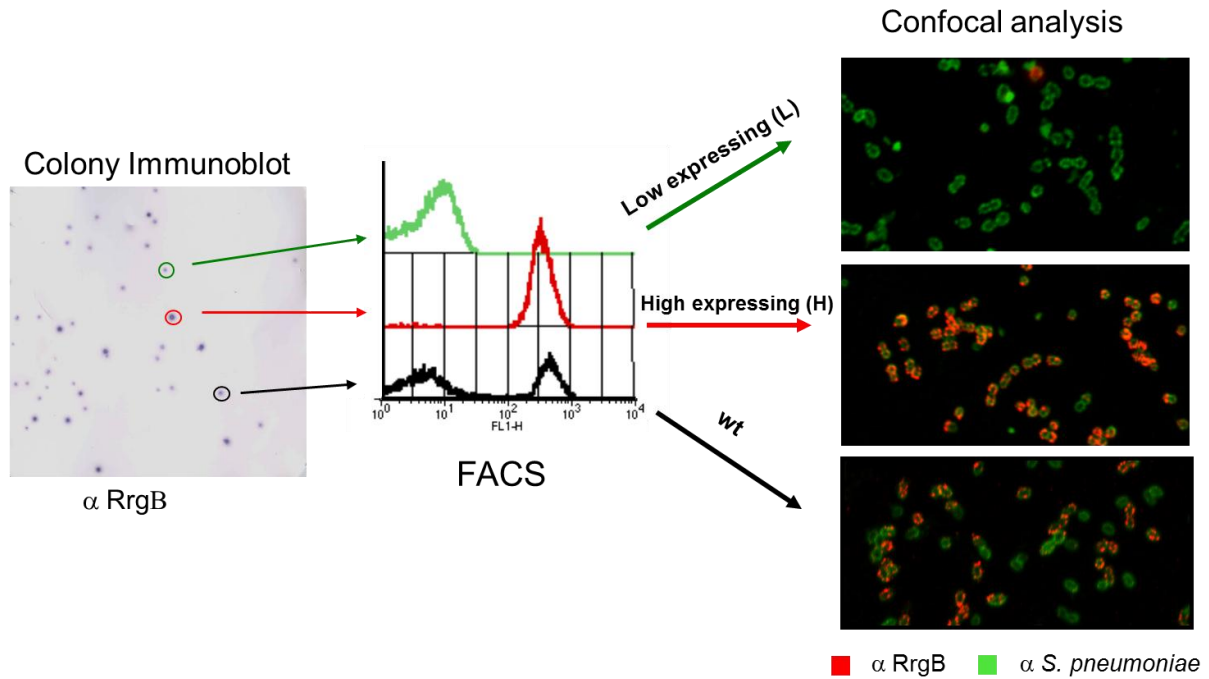


Fig. 8 Pilus1 displays a biphasic expression pattern. By colony immunoblotting using anti-RrgB antibodies the level of pilus expression was analysed. Green, red and black circles relate with colonies displaying low, high or medium pilus expression respectively. Each colony was grown and recovered bacteria were stained with anti-RrgB antibodies and analyzed by flow cytometry. The three populations identified by FACS, population L (low pilus expression), H (high pilus expression) and wt (medium pilus expression), were also stained for immunofluorescence study (anti-RrgB in red and anti-capsular in green) (Image redrawn from De Angelis et al., 2011).

Role of S.pneumoniae pilus1

Different studies demonstrated that pneumococcal adherence to human epithelial cells and subsequent ability to cause invasive disease is enhanced by expression of pilus1 (Nelson et al., 2007; Barocchi et al., 2006). In addition, PI-1 deletion mutants are also less virulent in murine models of colonization, bacteremia and pneumonia. Pilus1 expression also enhances the host inflammatory response that might damage the mucosal barrier and facilitate the invasion and the severity of the disease (Barocchi et al., 2006, Nelson et al., 2007, Hilleringmann et al., 2008). It has been demonstrated that the component responsible for pilus1 adhesion is the ancillary protein RrgA. In particular, recombinant RrgA and purified pili adhered in *in vitro* assays to extra cellular matrix (ECM) components, like collagen I, fibronectin and laminin (Hilleringmann et al., 2008; Nelson et al., 2007; Hava et al., 2003;

Hava and Camilli, 2002). A recent report proposes a role for RrgA but not for the pilus structure “per se” during *in-vitro* biofilm formation, probably indicating a function for RrgA in bacteria-bacteria interactions (Munoz-Elias et al., 2008). Interestingly, all *Streptococcus pneumoniae* pilus1 components, RrgA, RrgB and RrgC were recently shown to elicit different degrees of protection from lethal challenge, both in active and passive immunization studies, in different mouse model of infection (intra-nasal, intra-peritoneal and intravenous challenge); the backbone RrgB resulted to be the most effective in the immunization experiments, therefore, despite the sequence variability and the limited coverage of these antigens, these proteins are currently evaluated as potential candidates to be included in a new protein based pneumococcal vaccine (Gianfaldoni et al., 2009). In particular, antibodies against pilus components have been shown to induce in vitro opsonophagocytic killing (Harfouche et al., 2012). Based on the information concerning the role of pili in pneumococcal adhesion to epithelial cells, the activity of anti-pilus antibodies in opsonophagocytic killing and the characterization of RrgA as pilus adhesin, the main focuses of this work have been:

- To better define the contribution of *S. pneumoniae* type-1 pili in adhesion to human epithelial cells
- To investigate if anti-pilus1 antibodies are also able to prevent bacterial adherence to human epithelial cells
- To identify the portion of the RrgA molecule responsible for the adhesion to human epithelial cells.

Material & Methods

Bacteria strains and growth conditions

In this work were used *Streptococcus pneumoniae* strains belonging to different serotype: TIGR4 strain (serotype 4), 6B Finland12 and 6B SPEC strains (serotype 6B) and 19F Taiwan14 strain (serotype 19F). *S. pneumoniae* strains were routinely grown over-night (ON) at 37°C in 5% CO₂ on Tryptic Soy Agar plates (TSA) (Becton Dickinson) supplemented with 10 mg/L colistine, 5 mg/L oxolinic acid, and 5% defibrinated sheep blood. Liquid cultures were carried out statically at 37°C under 5% CO₂ humidified atmosphere until A₆₀₀ = 0.4 in Todd Hewitt Broth supplemented 0.5% (w/w) yeast extract (THYE, Becton Dickinson) unless otherwise specified.

Cell culture techniques

In this study were used a panel of human cell lines such as cervical (ME180), pulmonary (A549 and Calu-3) and canine kidney (MDCKII) epithelial cells. All cell lines were purchased from the American Type Culture Collection (ATCC). Epithelial cells were maintained in growth medium described in Table 1 and incubated at 37°C in 5% CO₂. All cell culture reagents were purchased from Gibco/Invitrogen.

Table 1 Medium composition for cell culture.

Medium Composition			
ME180 cells	A549 cells	Calu-3 cells	MDCKII cells
RPMI 1640	RPMI 1640	DMEM (4.5g/L D-Glucose)	DMEM (1g/L D-Glucose)
10% heat-inactivated fetal bovine serum	10% heat-inactivated fetal bovine serum	10% heat-inactivated fetal bovine serum	10% heat-inactivated fetal bovine serum
antibiotics 100X	antibiotics 100X	antibiotics 100X	antibiotics 100X
0.4mM CaCl ₂			

Adhesion assay

Epithelial cells were grown in 24 well plates up to fully confluent. Before use, the monolayers were washed twice with PBS. *S. pneumoniae* bacteria were grown to mid-log phase ($OD_{600} = 0.4$) and then resuspended in infection medium (basal medium without antibiotics) supplemented with 2% fetal bovine serum. Bacterial suspensions were applied to cell monolayers with a multiplicity of infection (MOI) of approximately 100 bacteria/cell. At the end of a 1 hour incubation period at 37°C in 5% CO₂, wells were washed four times with PBS to remove non-adherent bacteria, and the total number of colony-forming units (cfu) was estimated after addition of PBS 0.1% TRITON to the well's contents. Adhesiveness was quantified by determining the ratio of cell-associated colony-forming units versus total colony-forming units present in the assay.

Adhesion inhibition assay

To investigate the role of anti-pilus antibodies in preventing bacterial adherence to host cells, we performed adhesion assay as previously described with some modifications. Before infecting cells, bacteria were pre-incubated for 30 minutes at 37°C in 5% CO₂ with polyclonal or monoclonal antibodies against pilus components. Bacteria were then washed twice with PBS, resuspended in infection medium and used in the adhesion assay.

Confocal immunofluorescence microscopy

ME180 cells were cultured on Falcon transwell filters (pore size 0.4µm) in 24-well dishes up to fully confluent. *S. pneumoniae* bacteria were grown up to $OD_{600} = 0.4$, resuspended in infection medium and cells were infected with at an MOI of 100:1 bacteria/cell. At the end of a 1 hour incubation period at 37°C in 5% CO₂, cells were washed four times with PBS to remove non-adherent bacteria, and fixed in 1% formaldehyde for 20 minutes at RT. After fixing, the PET membrane supporting the cells was cut and inserted into a multiwell plate where was blocked (blocking solution, Duolink II) for 20 minutes at RT. Samples were then stained with primary antibody diluted in PBS 0.1% TRITON 1% BSA for 15 minutes at RT. The staining was performed using rabbit omni serum to identify the capsule and mouse anti-RrgB antibodies against the backbone of pilus1. After incubation with primary antibody the membranes were washed two times in PBS-T (PBS 0.1% TRITON) and incubated with goat anti-rabbit and goat anti-mouse Alexa Fluor-conjugated secondary antibodies (excitation at 568nm and 488nm, respectively), plus phalloidin conjugated with Alexa Fluor dye A₆₄₇ to

stain F-actin. Slow Fade reagent kit was used to mount cover slips. The slides were analyzed with a Zeiss LSM710 confocal scanning microscope.

Immunogold labeling and Electron microscopy

In order to analyze the amount of capsule among different serotype of *S. pneumoniae* strains, we applied the lysine-acetate-based formaldehyde-glutaraldehyde ruthenium red-osmium fixation procedure (LRR fixation) (Hammerschmidt et al., 2005). Bacteria were grown in THYE at 37°C up to OD₆₀₀ = 0.4, centrifuged for 5 min at 3500 rpm (RT), washed once with PBS and fixed for 20 min on ice. The fixation solution containing 2% paraformaldehyde and 2.5% glutaraldehyde in cacodylate sucrose buffer (0.1 M cacodylate, 0.01M CaCl₂, 0.01M MgCl₂, 0.09M sucrose; pH 6.9) in the presence of 0.075% ruthenium red and 0.075M lysine acetate to preserve the capsule. The samples were washed twice for 30 min on ice with cacodylate buffer containing 0.075% ruthenium red and then fixed a second time with 2% formaldehyde and 2.5% glutaraldehyde in cacodylate buffer with 0.075% ruthenium red overnight on ice. After inclusion in resin, bacterial pellets were cut with an ultramicrotome and sections examined using an electron microscope in collaboration with Dr.ssa Annarita Taddei (La Tuscia University, Viterbo).

To both visualize pili and the capsule, bacteria were grown up to OD₆₀₀ = 0.4, centrifuged for 5 min at 3500 rpm, resuspended in 1ml of PBS and incubated for 20 min on ice. Bacteria were then centrifuged for 1 min at 13000 rpm and resuspended in blocking solution (PBS 0.1% BSA) for 15 min. After incubation, primary antiserum against RrgB diluted 1:25 was added for 1 hour at RT. The samples were washed twice with blocking solution and incubated with secondary antibody conjugated to 5-nm gold particles diluted 1:100 in PBS 0.1% BSA for 1 hour at RT. Bacteria were then washed three times with blocking solution and processed for capsular detection as described above.

Moreover, to visualize the interaction of piliated bacteria with epithelial cells, ME180 cells were cultured on Falcon transwell filters (pore size 0.4µm) in 24-well dishes up to fully confluent. Bacteria were grown up to OD₆₀₀ = 0.4, suspended in infection medium and cells were infected with at an MOI of 100:1 bacteria/cell. At the end of a 1 hour incubation period at 37°C in 5% CO₂, cells were washed four times with PBS to remove non-adherent bacteria. The PET membrane supporting the cells was then cut and fixed with 2.5% paraformaldehyde + 2.5% glutaraldehyde in cacodylate sucrose buffer (0.1 M cacodylate, 0.01M CaCl₂, 0.01M MgCl₂, 0.09M sucrose; pH 6.9). After fixing, the membrane was processed and analyzed

using a focused ion beam scanning microscope (FIB) in collaboration with Dott. Andrea Di Giulio (LIME, Roma3 University).

Genomic DNA extraction

Genomic DNA extractions were performed from 10 ml of bacterial liquid culture grown until final OD₆₀₀ 0.7 - 0.8. Cells were harvested by centrifugation, suspended in 170µL of TET buffer (20mM TRIS pH 8, 2mM EDTA, 1% Triton X-100, Sigma) plus 5µL 10 U/mL mutanolysin (Sigma) and incubated at 37°C for 1 h. Subsequently, 25µL of Proteinase K (20mg/ml) (Sigma) were added and the mixture was incubated at 56°C for 1-2h until complete clearing of the lysate. Then 10µL of RNase A (10 mg/ml) (Sigma) were added and incubate at the same temperature for additional 10 min. Genomic DNA from the bacterial lysate was purified with Nucleospin[®] Tissue (Macherey-Nagel) according to manufacturer's instructions. Briefly, this includes 10 min incubation after the addition of 200µL of B3 buffer, followed by the addition on 210 µL of Ethanol. Sample was vortexed and transferred to NucleoSpin[®] column. The column was spinned at high speed in a bench microfuge. The flow-through was discharged, and two subsequently wash steps were performed using 500µL of BW buffer and 600µL of B5 buffer. The column was then centrifugated 3 min at high speed to dry and genomic DNA was eluted with 200µL of pre-warmed BE buffer (70°C). Genomic DNA was spectrophotometrically quantified at 260 and 280 nm and visualized on a 1% agarose gel.

Construction of 19F Taiwan14 capsular deletion mutant

The entire capsule locus was deleted in 19F Taiwan14 strain by allelic exchange, according to the procedure described by Pearce et al., 2002. In *Streptococcus pneumoniae* strains the capsular genes were always located in a region of the chromosome comprised between dexB and aliA (Garcia et al., 1997; Pearce et al., 2002), two genes unrelated to capsule polysaccharide biosynthesis. To build the capsular mutant strain, a DNA fragment containing a kanamycin (Km) cassette was constructed. The DNA fragment contained an aphIII gene, conferring Km resistance, flanked by dexB (685 bp) and aliA (1268 bp) genes. The construct was assembled by using Splicing Overlap Extension (SOE) PCR (Heckman et al., 2007). pGEX plasmid from *Escherichia coli* was used as a template for aphIII gene amplification and chromosomal DNA of pneumococcal 19FTaiwan14 strain was used as a template for

amplifying *dexB* and *aliA* genes. PCR products were obtained by using three pairs of primers: respectively P1/P2 for *dexB*, P3/P4 for *aphIII* and P5/P6 for *aliA* (Table 2). P2/P3 and P4/P5 primers were designed to have overlapping flanking regions and the three PCR products were joined together to form the deletion fragment. The deletion fragment was subsequently used for pneumococcal transformation. To select bacterial clones in which the capsular genes were replaced with the resistance cassette, bacteria were plated on blood-agar plates with kanamycin (500µg/ml). The deletion of the capsular locus was confirmed by PCR and genomic sequencing analysis.

Table 2 Oligonucleotides used to amplify *dexB*, *aliA* and *aphIII* genes.

Primer name	Sequence 5'-3'
P1	GAACATATCGGTCTTCAGTATCAGGAAGGTCAGCC
P2	TTCACTGTTCGCGACTAAGGATACGCTTC
P3	TATCCTTAGTGCGGAACAGTGAATTGGAGTT
P4	GTCAACAGAATTGTTGCGGATGTACTIONCAG
P5	CATCCGCAACAATTCTGTTGACATCTTTCTGA
P6	CGCTGAACTTTTGTAGTTGCTGTTTGGTCAACTGG

Polymerase Chain Reaction (PCR)

High fidelity PrimeSTAR (Takara) DNA polymerase was used to yield high quantities of DNA for cloning purpose. Typically, 50µL of reaction mix contained 5X buffer plus Mg²⁺, 200µM dNTPs mixture, 20pmol primers, 50ng of genomic DNA template and 1.25U of polymerase enzyme. PCR program was set-up according to the following layout:

94°C	15 min	1 cycle
98°C	10 s	5 cycles
Oligo melting Tm1 72°C	15 s 1 min every 1 kb template	
98°C	10 s	30 cycles
Oligo melting Tm2 72°C	15 s 1 min every 1 kb template	
72°C	5 min final elongation	1 cycle
4°C	∞	

Tm1 indicates the melting temperature of the exact genomic-primer annealing region, while Tm2 represents the full-length oligonucleotide melting temperature.

5µL of the amplification reaction was mixed with 1µL of gel loading buffer (Sigma) and loaded on 1% agarose gel. Agarose powder (Sigma) was melted in 1X TAE buffer (400mM Tris-acetate, 10mM EDTA, Invitrogen) and before complete solidification an intercalating dye for UV visualization, SYBR® Safe DNA gel stain (Invitrogen) was added. Gels were run at 100 V constant and images were acquired by laser densitometry (Gel-Doc Imaging System). 1 Kb Plus DNA ladder (Invitrogen) was used to determine the right fragment size. PCR were purified according to QIAGEN PCR purification kit protocol, column elution was completed with nuclease-free water and purified DNA was spectrophotometrically quantified.

Streptococcus pneumoniae transformation

19FTaiwan14 strain was transformed with the capsular deletion fragment by using conventional methods (Alloing et al., 1998). Bacteria were grown in BHI (Brain Heart Infusion broth) at 37°C in 5% CO₂ until OD 0.1. After that competent bacteria were obtained by incubation with pre-warmed Competence Induction Medium (CIM) for 20 min at 37°C. CIM medium is composed of: 9ml BHI+ 1ml horse serum + 0.1ml 1M glucose + 1µl CSP (competence-stimulating peptide) isoform 1. After incubation, 3µg of PCR deletion fragment was added and incubated for 1h at 37°C. Bacterial suspension were then plated on TSA plus 500µg/ml kanamycin and incubated ON at 37°C.

Colony immuno-blot

Bacteria were diluted on blood-agar plates to obtain isolated colonies. Following ON growth, nitrocellulose membrane discs (Millipore) were gently placed on the plates, removed after 5 min, heat-treated with microwave irradiation (300 W for 2 min) and then processed for Western Blot analysis as described below.

Western blot analysis

The membrane was blocked for 1 h at RT in PBS containing 5% skim milk (Difco) and 0.1% Tween20 (Sigma-Aldrich) and subsequently incubated with anti-RrgB serum diluted 1:10000 in the same blocking solution. After washing with PBS-0.1% Tween20, membranes were

incubated with the HRP-conjugated secondary antibodies (DAKO) for an additional hour. The detection was performed by using ECL and/or 4-CN substrates (PIERCE and BIO-RAD, respectively).

Flow cytometry analysis

In order to evaluate the capacity of anti-RrgA mAbs to recognize the pilus ancillary protein on the bacterial surface, T4 sub-population H bacteria were grown overnight on TSA/blood plates, harvested and incubated with four different mouse mAbs against RrgA (23F2/13, 18C8/37, 18C8/5 and 11B9/61) at the concentration of 1 μ g of antibody for 10⁸ CFU of bacteria. Polyclonal anti-RrgA antibodies were used as a positive control (dilution 1:100). After labeling with a secondary PE-conjugated antibody (Jackson Laboratories, dilution 1:100), bacteria were fixed with 2% paraformaldehyde. Bacterial staining was analyzed by using a FACS-Calibur cytometer (Becton Dickinson).

Epitope mapping

The epitope-mapping approach was based on the method described by Peter and Tomer, 2001, which we adapted to the following two protocols (Soriani et al., 2010; Koehler et al., 2011):

1) *Immunocapturing of peptides from antigen partial digestion.* Peptide mixtures were obtained by digestion of RrgA with trypsin, GluC and LysC (independently) in 50 mM ammonium bicarbonate buffer in a ratio 10:1 at 37°C for 3 hr. To capture the epitope-containing peptide, a 25 μ l suspension of Dyanbeads Pan Mouse IgG (uniform, superparamagnetic polystyrene beads of 4.5 μ m diameter coated with monoclonal human antimouse IgG antibodies) was used. The beads were washed twice with PBS using a magnet and resuspended in the initial volume. One μ g of the probe (murine) mAb (23F2/13, 18C8/37, 18C8/5 and 11B9/61) was added and incubated for 30 min at room temperature, after which the beads were washed twice with PBS to remove mAb excess. 0.5 μ l of Protease Inhibitor Mix (GE Healthcare) were added prior to the addition of the peptide mixture to avoid potential degradation of the antibodies. The sample was incubated for 30 min at room temperature with gentle tilting and rotation. After incubation the beads were washed three times with 1 ml PBS, and the bound peptide was then eluted with 50 μ l of 0.2 % TFA. The elute fraction was concentrated and washed with C18 ZipTips (Millipore) and eluted in 3 μ l of 50 % ACN and 0.1 % TFA. For MALDI-MS analysis, one microliter of sample was mixed

with the same volume of a solution of alpha-cyano-4-hydroxy-transcinnamic acid matrix (0.3 mg/ml in H₂O:ACN:TFA at 6:3:1), spotted onto the MALDI target plate and allowed to air-dry at room temperature. MALDI mass spectra were recorded in the positive ion mode on an UltrafleXtreme MALDI TOF/TOF instrument (Bruker Daltonics). Ion acceleration was set to 25 kV. All mass spectra were externally calibrated using a standard peptide mixture. For MS/MS analysis, the MASCOT search engine (Matrix Science, London, UK) was used with the following parameters: one missed cleavage permission, 20 ppm measurement for MS and 0.3 Da for MS/MS tolerance. Positive identifications were accepted with p values lower than 0.05. In the searches, methionine residues modified to methionine sulfoxide were allowed.

2) *Partial digestion of immunocaptured antigens.* To allow the capture of conformational epitopes, the order of the steps in the previous protocol was inverted. The intact protein (20 µg) was added to the beads, allowing binding to the immobilized mAbs. The protease was then added to the sample in a ratio 50:1, with incubation at 37°C for 1h. After proteolysis, the beads were washed ten times with 1 ml PBS, and the bound peptide was then eluted as previously described. To avoid the analysis of proteolyzed antibody fragments within the elute fraction, negative controls were carried out where PBS was used instead of protein samples.

Results

Involvement of pneumococcal TIGR4 strain pili in the adhesion to different epithelial cells

To study the involvement of pilus components in the adhesion to epithelial cells, we compared levels of adherence to different epithelial cell monolayers by various pneumococcal strains selected for the differential expression of pili. We used a serotype 4 strain named TIGR4 as the reference strain. The percentage of piliated bacteria in this strain is about 30%. By single colony isolation, we were able to separate two distinct populations, one expressing pilus at high levels named TIGR4H (T4H) and the other one expressing pilus at low levels named TIGR4L (T4L) (De Angelis *et al.*, 2011). Indeed, TIGR4H population is about 100% piliated, while the TIGR4L bacterial population carries only approximately 5% of piliated microorganisms. TIGR4 isogenic mutant strains lacking pilus components RrgA (ancillary protein) and RrgB (backbone protein) were also used in these studies.

In order to test the adhesive attitude of TIGR4 derived strains, we selected a panel of epithelial cell lines differing for their anatomical origin and the capacity to constitute polarized monolayers. In particular we used ME180 (human cervical), A549 (human alveolar), MDCKII (canine kidney) and Calu-3 (human bronchial) epithelial cell lines. ME180 cell line is not able to form fully polarized monolayers resulting in a high exposure of basolateral spaces between the cells. On the contrary, MDCKII, Calu-3 and A549 cell lines give rise to differentiated monolayers where the cells are closely sealed by means of adherence and tight junctions.

To perform this assay we seeded $\sim 10^5$ cells/well in 24 wells plate. Cells were grown till confluence. Then cells were infected with a Multiplicity of Infection (MOI) of 100 CFU/well in infection medium in 200 μ l volumes. At the end of the incubation period at 37° in 5% CO₂ (v/v), wells were washed and the total number of colony forming unit (CFU) were estimated after addition of PBS 0.1% Triton to the well contents. Adhesiveness was quantified by determining the ratio of cell-associated CFU versus total CFU added at time zero.

Adhesion to ME180

We observed that pilus mutant strains and T4L strain were extremely less adhesive to ME180 monolayers if compared to the *wild type* strain while the TIGR4H strain was the most adhesive (Figure 9). These data indicated that the level of adhesion was directly related to the presence of type I pilus and of both its sub-units, RrgA and RrgB, on the bacterial surface.

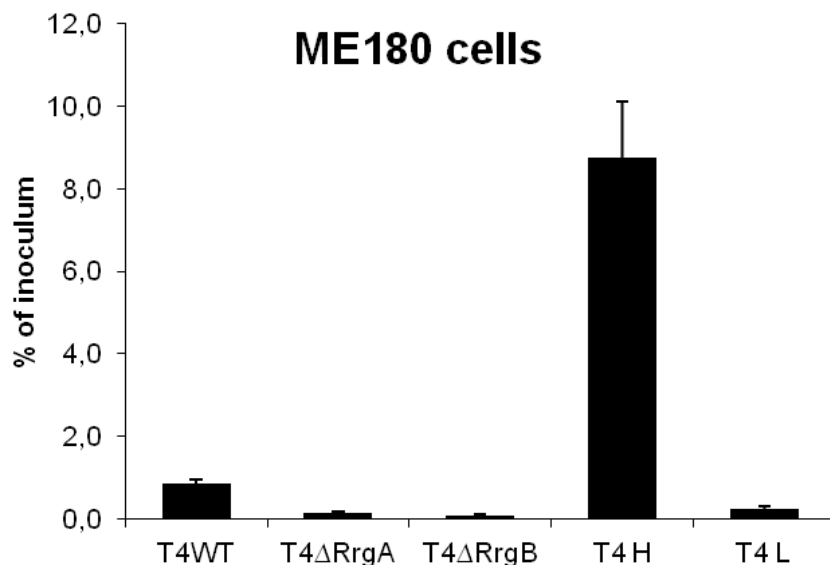


Fig. 9 RrgA and RrgB are involved in the binding of *S. pneumoniae* TIGR4 to ME180 epithelial cells. ME180 cells, grown to be fully confluent in a 24-well plate, were infected with the following pneumococcal strains for 1h: TIGR4 wild type, TIGR4H, TIGR4L, TIGR4ΔRrgA and TIGR4ΔRrgB. At the end of incubation, non adherent bacteria were gently washed off, and cells were lysed with PBS 0.1% Triton. Data are mean values \pm SD of three independent experiments.

Adhesion to A549, MDCKII and Calu-3

A similar behaviour was observed when using A549, MDCKII and Calu-3 cell lines even if we measured a decrease in the overall adhesion level respect to ME180 monolayers (Figure 10, 11, 12). Since A549, MDCKII and Calu-3 cells form intercellular junctions that prevent basolateral extracellular matrix components to be externally accessible, we hypothesized that the striking differences in adhesion between cell lines might depend on matrix exposure. This also supports the involvement of basolateral receptors as a ligand for pneumococcal type I pilus.

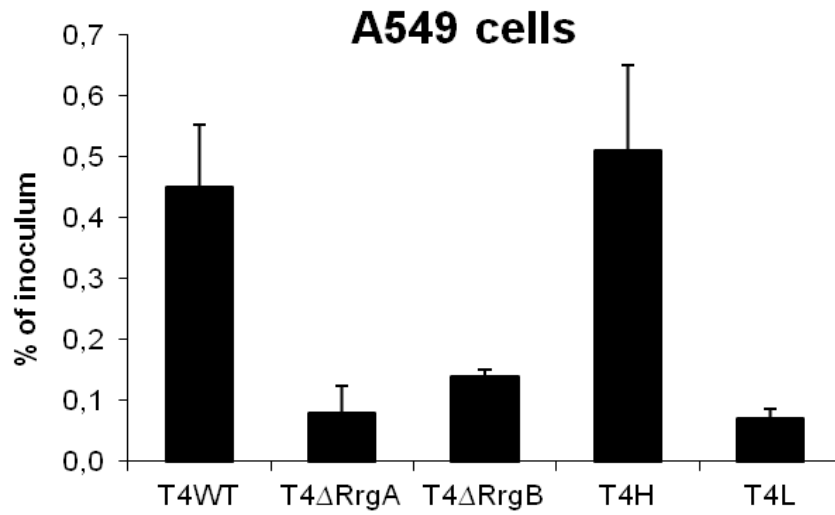


Fig. 10 Adhesiveness percentage of pneumococcal T4 strains to A549 cells.

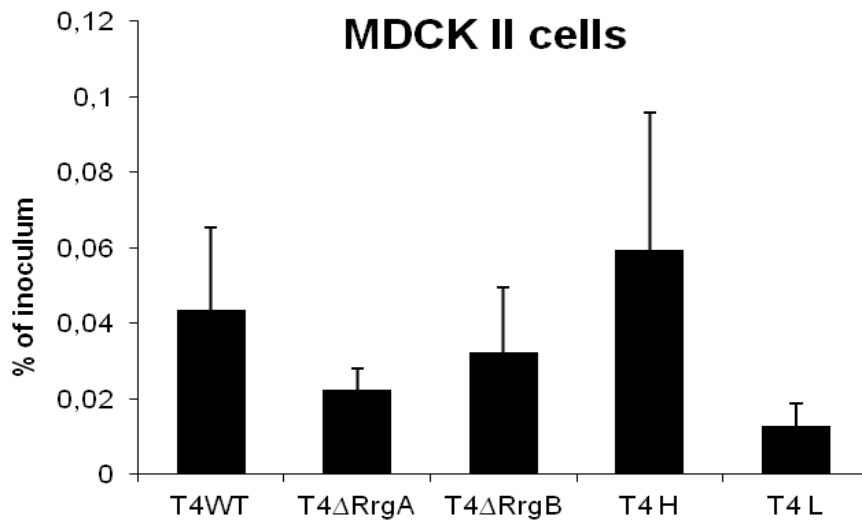


Fig. 11 Adhesion of T4 strains to MDCKII monolayers.

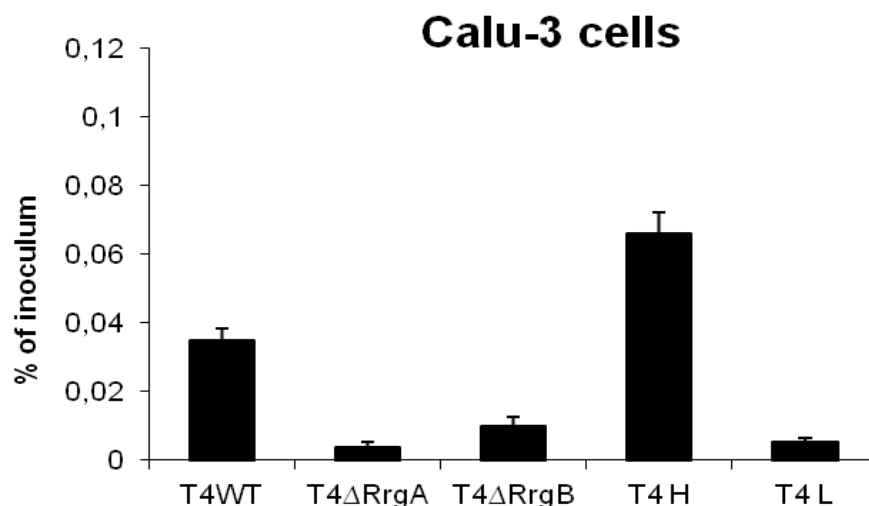


Fig. 12 Pneumococcal T4 strains adhesion to the Calu3 cell line.

Confocal microscopic analysis and electron microscopy studies using ME180 cell line confirms the contribution of pilus components to pneumococcal adhesion to epithelial cells

In order to better address the role played by *S. pneumoniae* pili in the adhesion to host cells we performed fluorescence microscopy experiments on ME180 monolayers infected with different T4 strains.

ME180 cells were grown on falcon polycarbonate transwell filters with 0.4 μ m pore size until fully confluent. Then we infected cells with T4 *wt*, T4H, T4L, T4 Δ *rrgA* and T4 Δ *rrgB* using a MOI of 100 CFU/cell as previously described. The filters were then fixed and incubated with specific antibodies against bacteria and pilus subunits. Primary antibodies revelation was achieved by using anti-mouse or anti-rabbit AlexaFluor-conjugated antibodies. Phalloidin-AlexaFluor647 was used for the staining of F-actin filaments in ME180 cells. Finally the filters were mounted on a glass slide and analyzed on a LSM710 confocal microscope.

As expected fluorescence data perfectly correlated with adhesion assay experiments. Indeed the number of piliated bacteria adhering to the monolayer was drastically greater compared to pilus mutants or non- piliated strain (figure 13). Furthermore bacteria seem adhere to the exposed basolateral surface of the ME180 monolayer confirming that the putative pilus ligand may reside in the extracellular matrix components.

Going deep in more structural details we were able to clearly visualize pili closely associated with the surface of epithelial cells (figure 14).

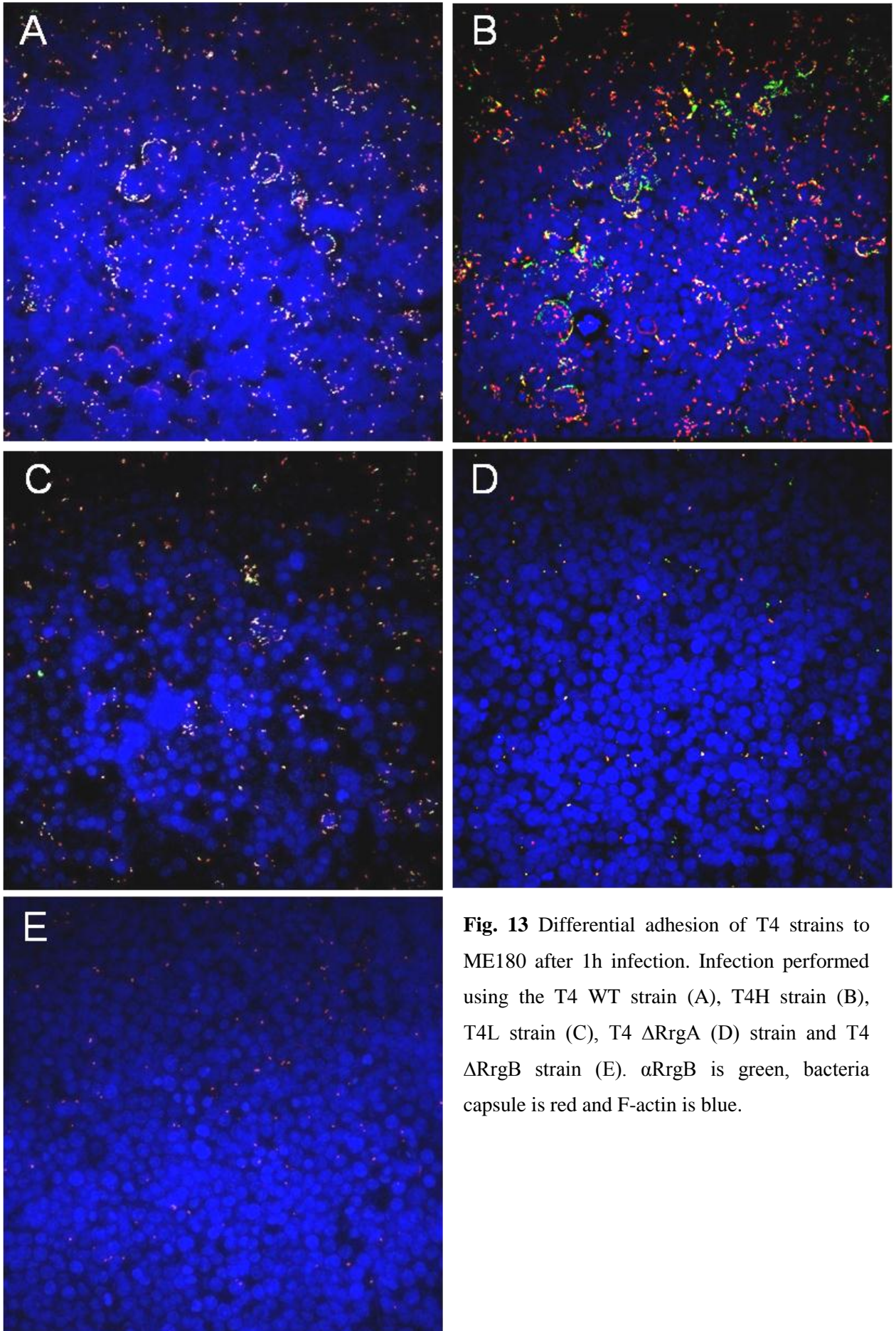


Fig. 13 Differential adhesion of T4 strains to ME180 after 1h infection. Infection performed using the T4 WT strain (A), T4H strain (B), T4L strain (C), T4 Δ RrgA (D) strain and T4 Δ RrgB strain (E). α RrgB is green, bacteria capsule is red and F-actin is blue.

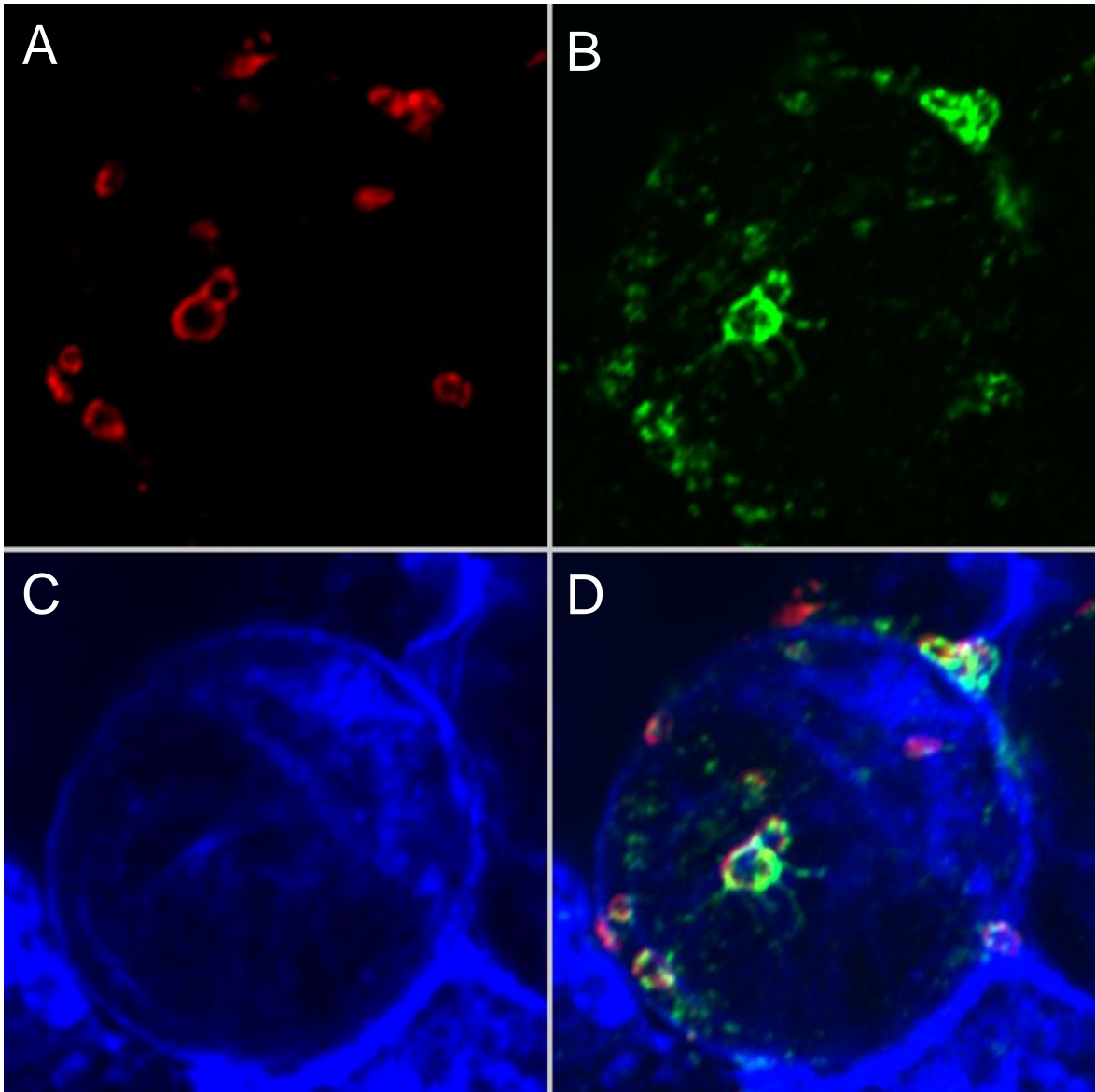


Fig. 14 This image was captured after infecting ME180 cells with pneumococcus T4 WT for 1h. In panel A is presented the capsule in red, panel B shows RrgB staining and panel C shows cellular F-actin. Panel D represents the merge of the three stainings.

Another important evidence was the fact that the great majority of adhering bacteria were piliated. Indeed when we infected ME180 monolayers with T4 *wt* almost all of adhering bacteria, were positive for pilus specific staining (figure 13 and 14).

Moreover to better visualize the interaction of piliated bacteria with epithelial cells, we performed electron microscopy studies on ME180 cells infected with TIGR H bacteria. To date this ME180 cells were grown on falcon polycarbonate transwell filters with 0.4 μ m pore

size until fully confluent and infected with T4 H as previously described in confocal analysis. After one hour of infection the filters were washed and fixed with 2.5% paraformaldehyde + 2.5% glutaraldehyde in cacodylate sucrose buffer. Filters were then processed and analyzed with focused ion beam (FIB) (in collaboration with Dott. Andrea Di Giulio, LIME).

As we can observe in Fig.15 (panel A) piliated bacteria adhere mainly at the level of the intercellular junctions where pili can reach the extracellular matrix components. Moreover a lot of bacteria were recovered all around cells that extrude from the monolayer (Fig. 15 panel B). These are death cells that, during the exfoliation, gradually detach from the epithelial layer and expose basolateral surface. These results confirm what we observed by confocal analysis that the putative pilus ligand may belong to the extracellular matrix components. Moreover this technic allows a good resolution visualizing of pili that extrude from bacterial surface and contact epithelial cells (Fig. 15 panel C).

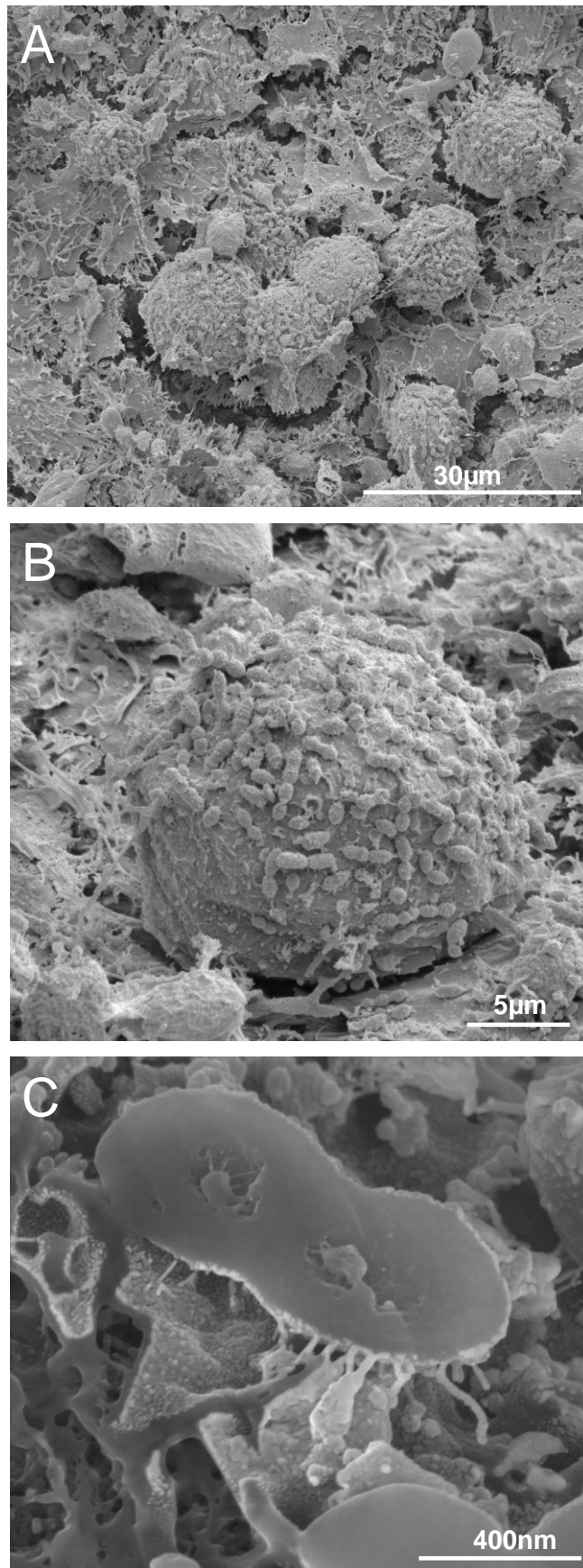


Fig. 15 FIB analysis of ME180 cells infected with T4 H at different enlargement (panel A, B and C).

Type I pilus mediated adhesion to cells varies among different *S.pneumoniae* strains

In order to study type I pilus-mediated adhesion in strains other than TIGR4, we test the adhesion abilities of a panel of strains belonging to different serotypes and characterized for having biphasic expression pattern of pilus 1. Indeed we selected a group of strains representative of common serotypes: 6B Finland12, 6B SPEC and 19F Taiwan14.

The adhesion assay was performed on ME180 cells as previously described and for each strain we analyzed the H and L subpopulation.

As shown in Fig. 16, difference in adhesion between H and L sub-populations was notice for all the strains tested but was extremely evident only when using T4 strain. These data suggest that although pili mediate adhesion, their contribution is variable among different strains. Moreover we observed that TIGR4 derived sub-population H display a higher capability to adhere with respect to the pilus-enriched populations of the other strains, suggesting that there probably exist different factors to cell adhesion that may modulate the contribution of these structures to cellular adhesion, such as capsule thickness.

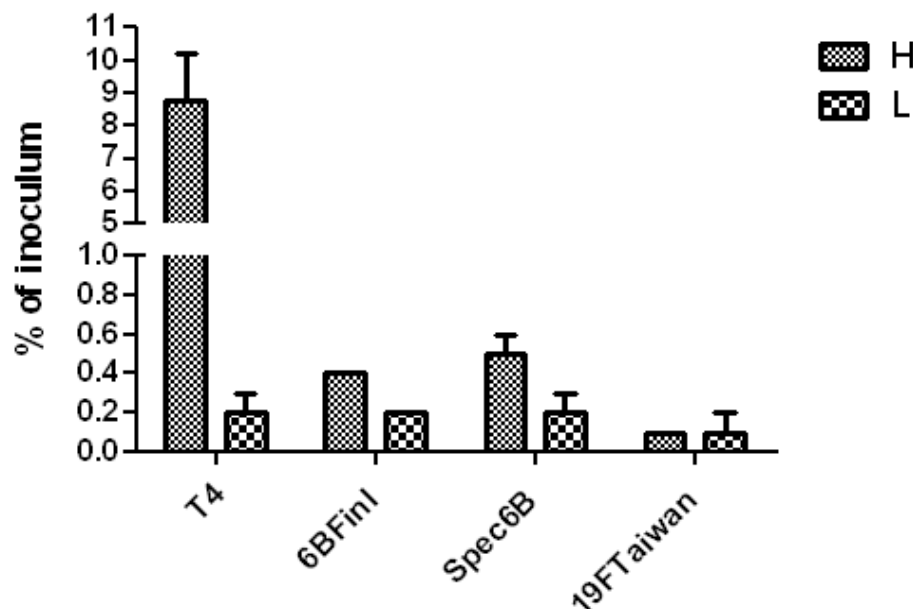


Fig. 16 Adhesion of piliated and non-piliated *S.pneumoniae* strains to ME180 cells.

Pilus dependent adhesion to host cells is modulated by capsule thickness

Based on the data previously reported, we hypothesized that the differences in adhesion between the T4 piliated bacteria and the other piliated strains may depend on the surface exposure of pili. To verify this hypothesis we analyzed the amount of the capsule in all the strains used in the adhesion assay by transmission electron microscopy studies (in collaboration with Dr.ssa Annarita Taddei of La Tuscia University, Viterbo). Bacteria were grown in THYE and fixed with 2% paraformaldehyde + 2.5% glutaraldehyde in the presence of 0.075% ruthenium red and 0.075M lysine acetate to preserve the capsule.

The results indicate that the capsule does not vary among H and L subpopulations of the same strain (data not shown). On the contrary, as shown in Fig. 17, there are considerable differences in capsule thickness among the strains tested. Whereas the T4 strain has a very thin capsule, particular almost all strains showed a very thick capsule (especially the 19F Taiwan14 strain). By comparing electron microscopy data with adhesion studies we found a clear correlation between capsule thickness and bacterial adhesion. Indeed bacteria harboring a thin capsule, as the T4 strain, showed the best adhesion to ME180 cells, while highly capsulated strains, poorly exposing pili, had a reduced capacity to adhere to host cells. These results indicate that the capsule thickness is inversely related with the bacterial ability to adhere to host cells likely due to the different exposure of pili on the bacterial surface.

In order to visualize both capsule and pili on the surface of bacteria, we performed Immuno Electron Microscopy studies on a highly capsulated strain like 19F Taiwan14 H. Bacteria were pre-incubated with a specific anti-RrgB serum and with a secondary antibody conjugated to 5nm gold particles. Bacteria were then fixed and processed as described above to preserve the capsule. As shown in Fig.18 only the portion of pili extruding from the capsule seems to be accessible to the antibodies, suggesting that the pilus contribution in adhesion should rely on the portion extending from the capsule.

To prove this hypothesis, we generated an isogenic capsular mutant on 19F Taiwan14 strain (19F Taiwan14 Δ cps) by in frame deletion of the entire capsular locus. Given the biphasic expression pattern of pili in *Streptococcus pneumoniae*, we isolated the sub-populations H and L from the 19F Taiwan14 Δ cps strain and we tested them in adhesion assays using ME180 cells. As shown in Fig.19, there were no significant differences in adhesion between the two sub-populations derived from the 19F Taiwan14 strain. On the contrary capsule deletion resulted in marked difference between piliated and not piliated sub-populations. These results support

the hypothesis that the capacity of pneumococcal strains to associate to host cells depends on the portion of pili extruding from the bacterial capsule.

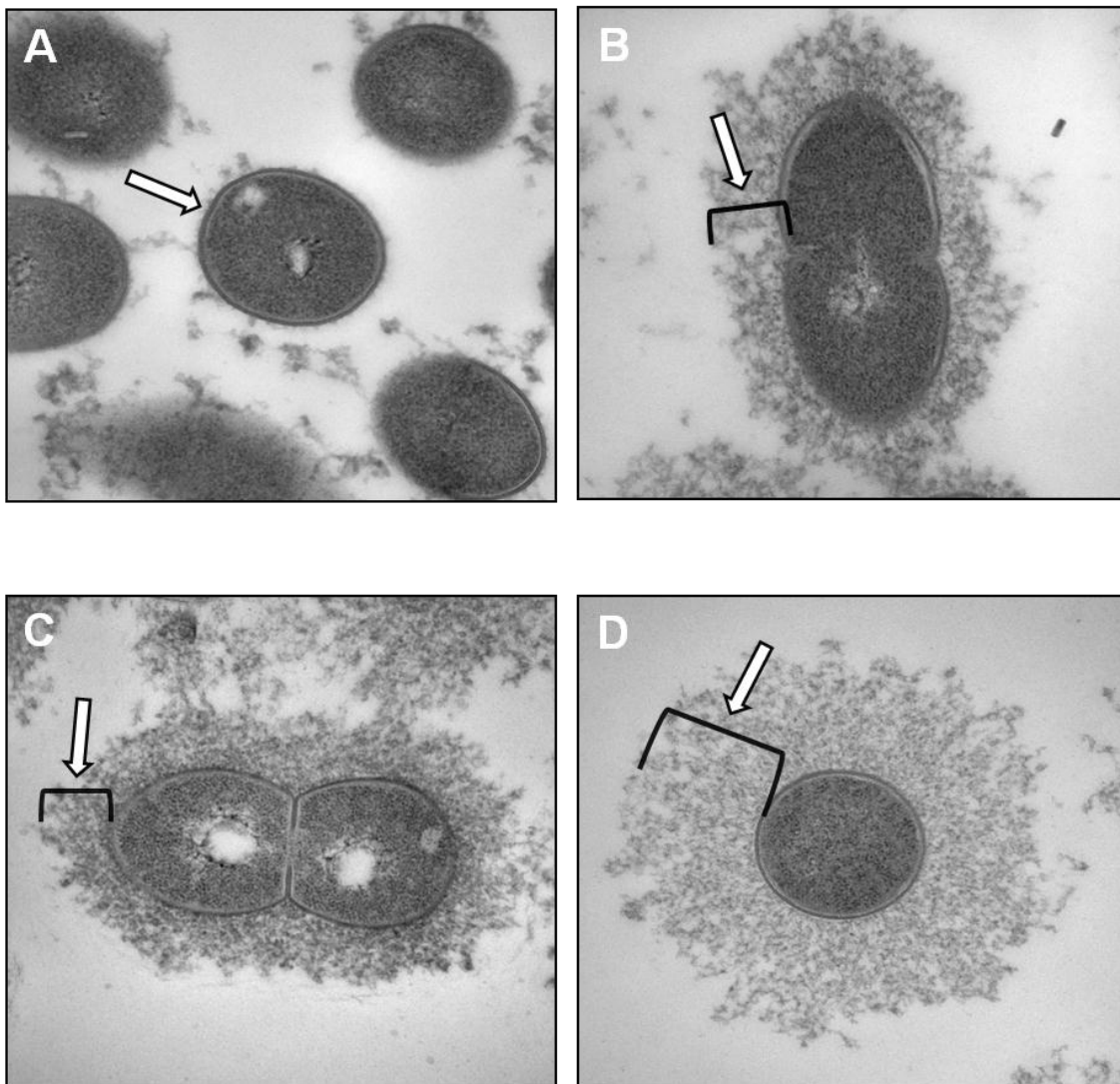


Fig. 17 EM analysis of the: (A) TIGR4 H, (B) 6B Finland12 H, (C) 6B SPEC H, (D) 19F Taiwan14 H. White arrows indicate the capsule.

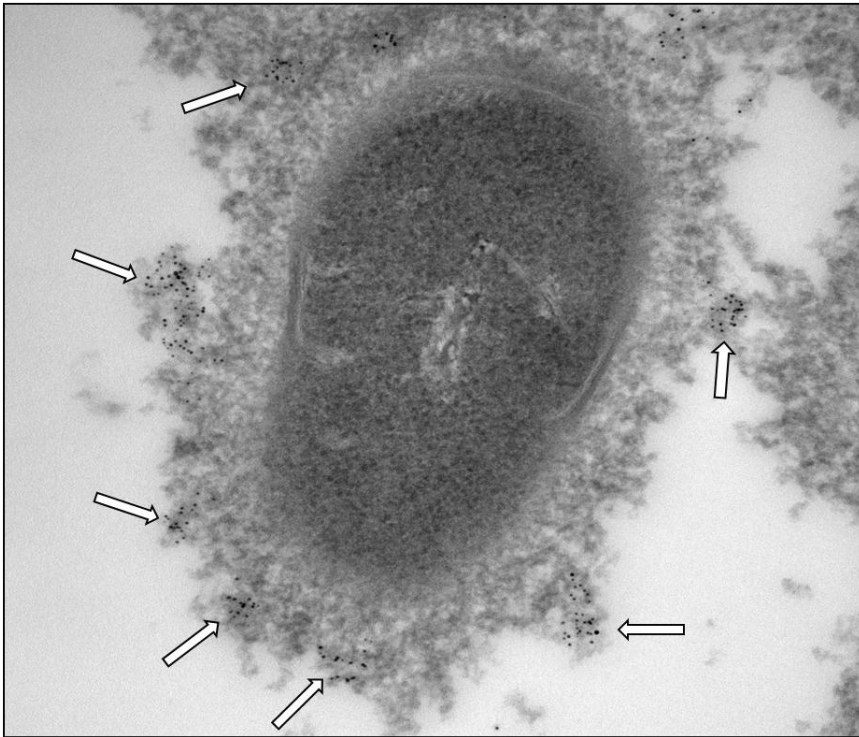


Fig. 18 Immunogold labeling of 19F Taiwan14 H pili. Bacteria were pre-incubated with a specific anti-RrgB polyclonal antibody for 1 hour at RT and with a secondary antibody conjugated to 5nm gold particles. White arrows indicate pili.

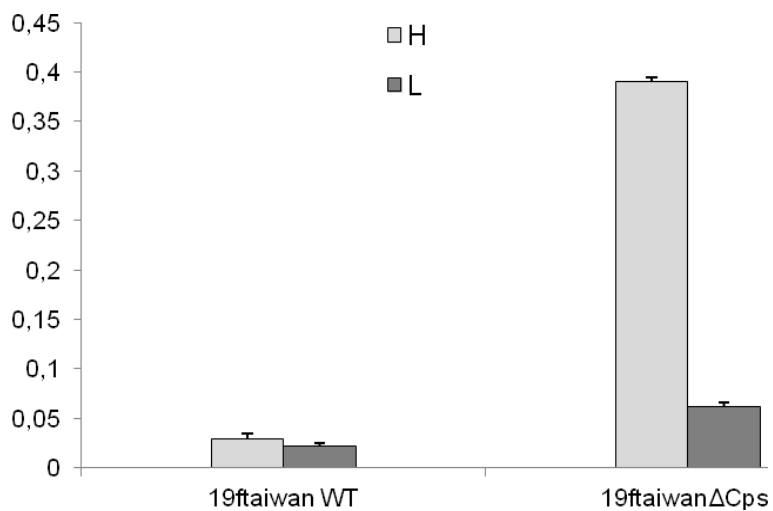


Fig. 19 Capsular locus deletion in 19FTaiwan strain results in increased pilus-dependent adhesiveness to epithelial cells.

Antibodies against pilus components reduce the capacity of piliated bacteria to adhere to the epithelial monolayer

It is known that anti-pilus antibodies are functional in inducing *in vitro* opsonophagocytic killing and that immunization with pilus subunits shows protection against pneumococcal infection in mice (Gianfaldoni *et al.*, 2007; Harfouche *et al.*, 2012). Given the above stated results revealing the role of pili in adhesion in strains where pili were prominently extruded from the capsule, it was rational for us to check if anti-pilus antibodies could also have a role in preventing pneumococcal adherence to epithelial cells.

To investigate this hypothesis, we realized an *in-vitro* adherence model on ME180 cells where anti-pilus antibodies were used at different concentrations. As a model strain we used the TIGR4 sub-population H that we previously characterized to be highly adhesive on ME180 cells.

Bacteria were pre-incubated with antibodies directed against pilus components RrgA or RrgB for 30 minutes. As negative controls we used bacteria incubated with PBS and bacteria incubated with antibodies specific to an unrelated surface-exposed protein (β -galactosidase bgaA) (Fig.20).

After pre-incubation with antibodies, bacteria were washed twice and used in the adhesion assay. The results showed that both α RrgA and α RrgB antibodies impaired bacterial adhesion when used at the highest concentration. Of interest, anti-RrgA antibodies were able to inhibit adhesion in a dose-dependent manner while preincubation with anti-bgaA antibodies had no effect on bacterial adhesion, excluding an aspecific effect due to antibody steric hindrance.

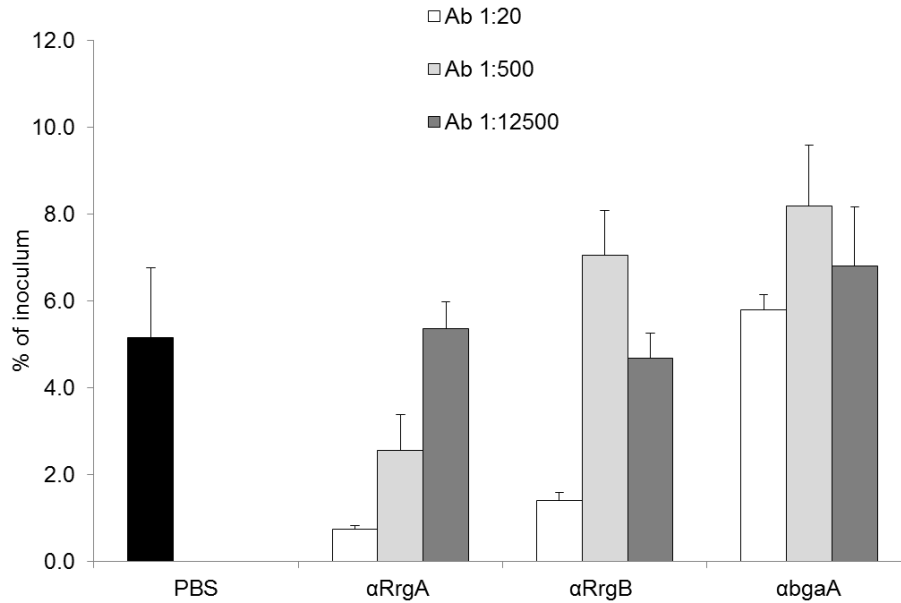


Fig. 20 Effect of anti-pilus antibodies on *Streptococcus pneumoniae* adhesion. T4H bacteria were pre-incubated with specific anti-sera against single pilus components (RrgA, RrgB) or with PBS and anti-sera against unrelated surface-exposed protein (bgaA) as a negative controls.

On the basis of the results observed using polyclonal antibodies, we decided to test also monoclonal antibodies against the pilus adhesin RrgA in inhibiting bacterial adhesion.

TIGR4 strain sub-population H bacteria were pre-incubated with 4 different monoclonal RrgA antibodies (IgG1) indicated as 11B9/61, 18C8/5, 18C8/37 and 23F2/13. PBS was used as negative control, whereas polyclonal RrgA antibody was used as a positive control (Fig. 21). The assay was performed as previously described. The results indicated that only the monoclonal antibody 11B9/61 had a strong effect in inhibiting bacterial adhesion. The fact that such a drastic effect is obtained using a monoclonal antibody suggests that a very limited portion of the RrgA molecule is in charge of mediating pilus mediated adhesion to ME180 cells.

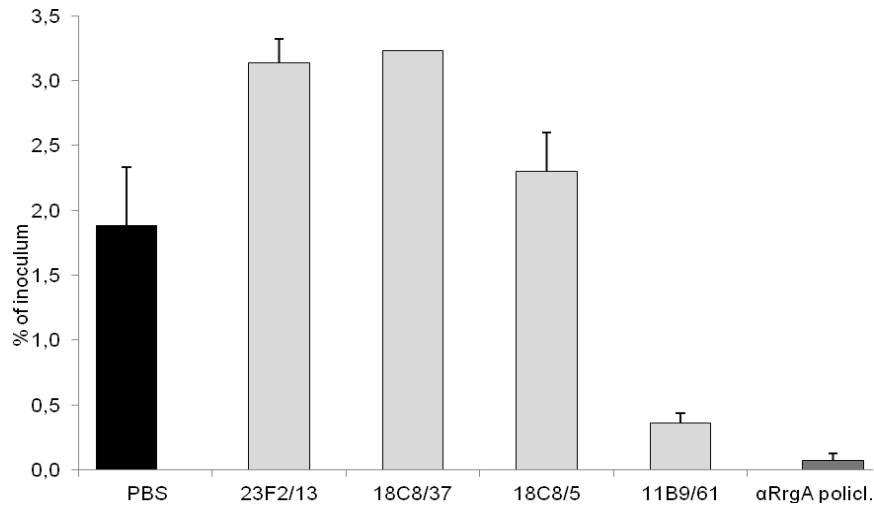


Fig. 21 Effect of monoclonal antibodies against RrgA on *S. pneumoniae* adhesion to ME180 cells. T4H bacteria were pre-incubated with four different anti-RrgA monoclonal antibodies at the concentration of 1 μ g mAb for 10⁸ CFU of bacteria. As a positive control bacteria were pre-incubated with polyclonal anti-RrgA antibodies and as a negative control bacteria were incubated with PBS alone.

FACS analysis shows that anti-RrgA mAbs binding to T4 H correlates with inhibition of adhesion

In order to elucidate the ability of the monoclonal antibodies against RrgA to recognize the protein on the bacterial surface, T4 subpopulation H bacteria were grown in liquid culture, incubated with each monoclonal antibodies and then analyzed by flow cytometry (FACS).

Interestingly, the analysis revealed that mAbs binding to RrgA on the bacterial surface was proportional with their ability to inhibit adhesion. In particular mAb 11B9/61, responsible for the greater inhibition of pneumococcal adhesion, resulted to be the most positive (Fig.22).

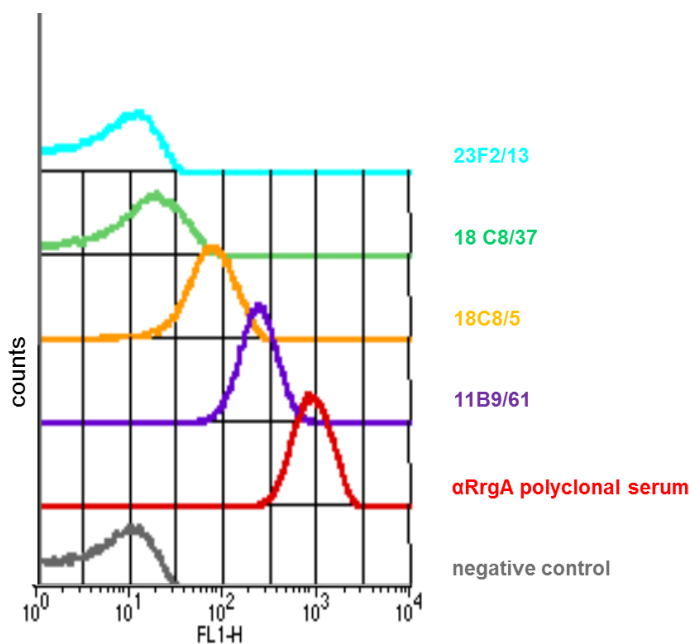


Fig. 22 FACS analysis with monoclonal antibodies against RrgA using TIGR4 sub-population H. Polyclonal antibodies against RrgA were used as a positive control.

Epitope mapping studies identify a variable loop in domain 3 of RrgA as the putative target for mAb 11B9/61

Given the reported results about the involvement of the monoclonal antibody 11B9/61 in inhibiting bacterial adhesion, we decided to perform epitope mapping studies on RrgA to identify the region involved in the binding of cellular ligands (this analysis was performed by Mario Ferrer Navarro - Universitat Autònoma de Barcelona).

A number of methods for the identification of epitopes are available. The most precise method, providing the structural details of the antigen-antibody interaction, is X-ray crystallography, but this is also the most labor intensive method and crystals of the complex cannot be always obtained. Other methods, like Pepscan (Geysen et al., 1987) and phage display libraries (Scott et al., 1990) have been useful for rapid epitope determination. The Pepscan technique uses sets of overlapping peptides, which must cover the entire sequence of a protein if the epitope region is totally unknown. This makes the technique very expensive and dependent on the purity of the synthesized peptides. Epitope mapping with phage-display libraries involves the display of random peptide sequences on the surface of filamentous bacteriophages. Neither method, however, is suitable for the detection of conformational or post-translationally modified epitopes.

As the use of a synthetic peptide library failed in the detection of the RrgA epitope recognized by the monoclonal antibodies, an approach suitable for the detection of conformational epitopes has been used. This approach involves proteolytic digestion of the target antigen prior (for lineal epitopes) or following (for conformational epitopes) immunocapturing and the subsequent analysis of the antibody-bound peptides by mass spectrometry (MS). In order to confirm the results obtained with the Pepscan approach the MS protocol for lineal epitopes was first performed, detecting no bound peptides. In contrast, application of the MS protocol for conformational epitopes led to the detection of a bound peptide, thus confirming the structural nature of the epitope. For the antibody 11B9/61, a single peptide was identified (Fig. 23), with a m/z of 2306.210 Da. The sequence of this peptide was first obtained by peptide mass fingerprinting and then confirmed by MS/MS, and corresponds to the segment 477-AAGYAVIGDPINGGYIWLNR-497. The length of the peptide is determined by the action of the proteases and the segment can only be said to contain the key residues of the epitope.

This peptide is located in domain 3 (Lys219-Ile586), which contains a region whose fold highly resembles that of the human A3 domain of von Willebrand factor (VWA), a molecule shown to interact with collagens I and III (Cruz et al., 1995). The VWA fold has been found in many eukaryotic cell-surface proteins involved in interactions with the extracellular matrix, including the β domain of integrins, where it has been shown to play a role in collagen interaction. RrgA's integrin I-like domain carries two insertion regions or “arms” that extrude from the core of the domain. The first of these regions involves residues Phe280-Asp318. The second, larger region ranges from Met392 to Gly516 and carries the epitope recognized by mAb 11B9/61 (Fig. 24.A). Interestingly, sequence analyses and structural predictions of RrgA homologs in different pathogenic streptococcal species showed that these proteins display a sequence identity level of approximately 50% (with similarity levels beyond 70%), and also harbor integrin I-like domains decorated with arms. It is precisely in the inserted arms that the sequence identity level is the lowest. This suggests an involvement of these regions in pathogenesis (Izoré T et al., 2012). Visual inspection of the identified peptide in the protein structure shows that the side chains of residues between Ala481 and Asn495 are the most accessible at the surface of the protein (See figure 24.B).

The other mAbs (23F2/13, 18C8/37, 18C8/5), with no neutralizing capabilities, recognize a different region in domain 3. The peptide bound these mAbs has a m/z of 3884.25 corresponding to the sequence 381-VIFHITDGVPTMSYPINFNHATFAPS YQNQLNAFFSK-417 of RrgA (Fig. 24). No MS/MS

spectra of this peptide could be obtained due to its high molecular weight and the low intensity signal detected in the mass spectrometer.

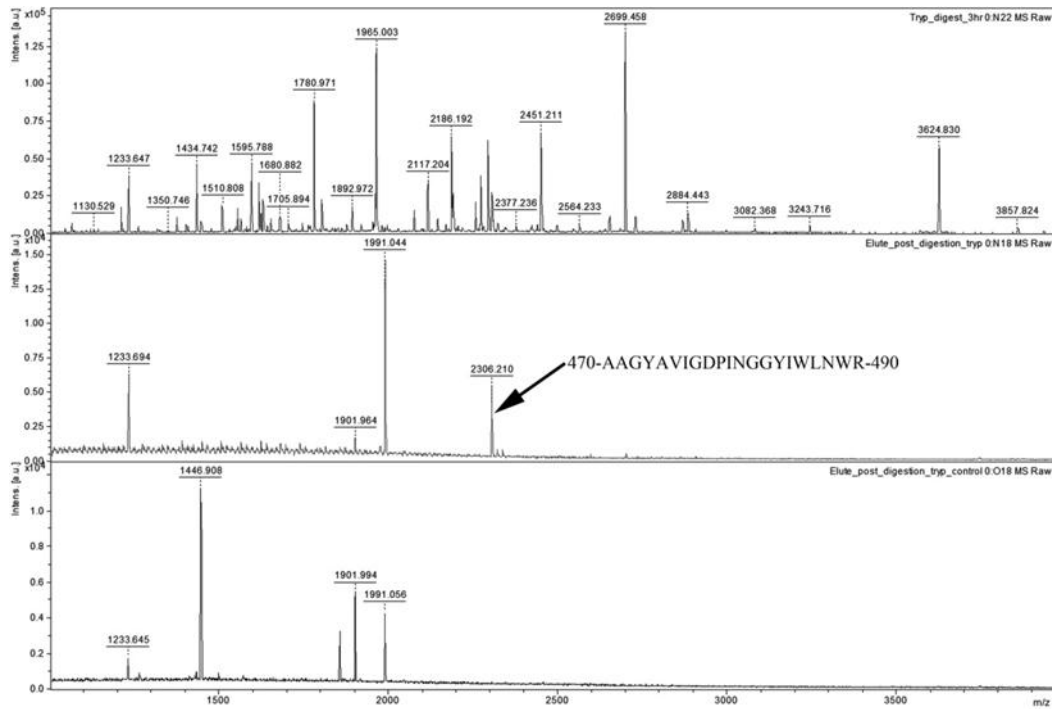


Fig. 23 MS spectra obtained for the epitope mapping of mAb 11B9/61. The upper spectrum shows the tryptic digestion of RrgA. The middle spectrum shows the captured peptide, with a m/z of 2306.210, and peptides from the partial degradation of the antibody by the protease, as confirmed by the control spectrum (lower spectrum).

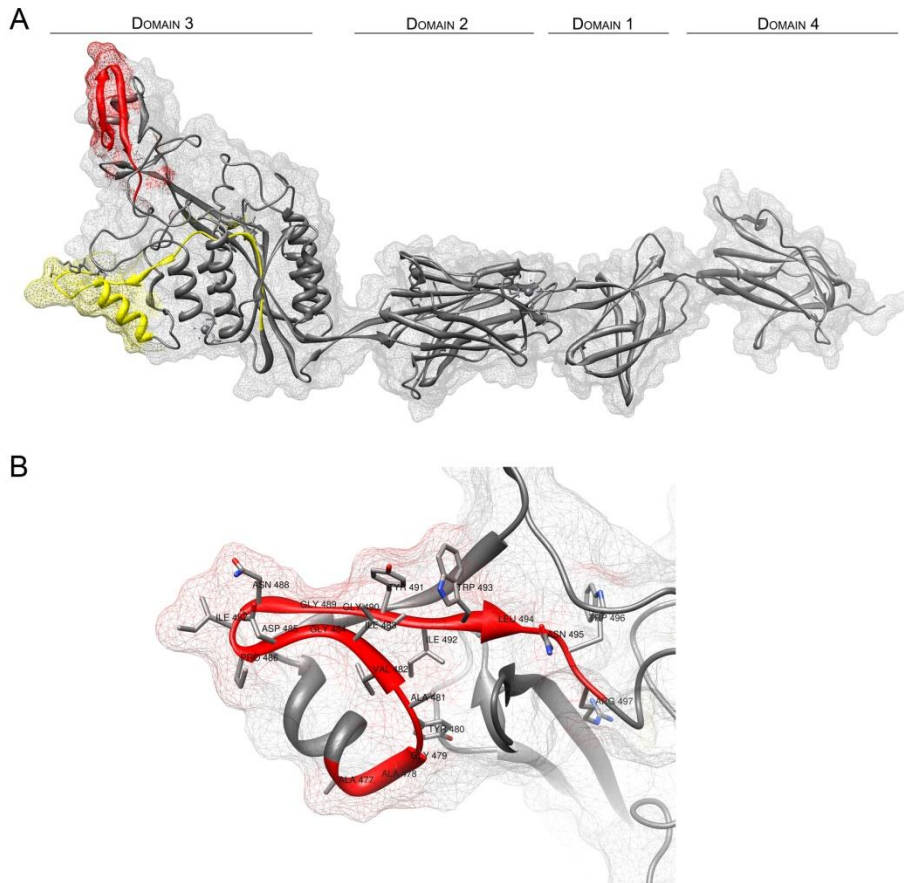


Fig. 24 Location of the identified epitopes in the structure of RrgA (pdb code: 2WW8). In red the region recognized by mAb 11B9/61. In yellow the region recognized by the mAbs 23F2/13, 18C8/37, 18C8/5.

Discussion and Conclusions

S. pneumoniae is a human pathogen able to cause both invasive and non-invasive diseases as well as to colonize the nasopharyngeal tract of children and adults. Thirty to 50% *S. pneumoniae* strains contain an islet (named pilus islet-1, PI-1) coding for a surface exposed pilus reported to be important both for colonization and virulence (Hava et al., 2002; Barocchi et al., 2006; Moschioni et al., 2008). Moreover, all the three pilus components (RrgA, RrgB and RrgC) are able to elicit protection *in vivo* and to induce a functional antibody response as demonstrated by active and passive immunization studies and by opsonophagocytosis assays performed with antisera raised against the pilus components. Pili were recently discovered in many gram-positive pathogens and, although their biological function has not been fully elucidated, their presence has been mostly related to bacterial adhesion, biofilm formation and translocation of host mucosal barriers (Barocchi et al., 2006; Manetti et al., 2007; Pezzicoli et al., 2008; Konto-Ghiorghi et al., 2009). In particular it has been clearly demonstrated that pilus component RrgA is the major determinant for adhesion to epithelial cells *in vitro* whereas RrgB is important to allow the formation of the polymeric structure into which the adhesin is incorporated (Nelson et al., 2007; Hilleringmann et al., 2008; Hilleringmann et al., 2009). In this work we aimed to better study the role of pilus components in adhesion to human epithelial cells and to evaluate the role of specific anti-pilus subunits antibodies in preventing such adhesion. Initially we found that the pilus-dependent bacterial adhesiveness to epithelial monolayers was reliant on the capacity of the cells to form intimate junctions. Indeed, among the epithelial cells tested, Me180 cervical epithelial cells, characterized to form weak adherence junctions, were the best model to study pneumococcal adhesiveness. This evidence led us to hypothesize that the pilus ligands, as already reported for other pilus-expressing gram positive bacteria, may reside in some of the extracellular matrix components rather than in cell associated receptors (Kreikemeyer et al., 2005; Hilleringmann et al., 2008; Banerjee et al., 2011). As a confirmation of this hypothesis immunofluorescence experiments showed that the majority of piliated bacteria were localized within the intercellular space or associated with cells extruding from the monolayer, thus exposing the basolateral surface. Once identified the most appropriate cellular model we started the characterization of pilus dependent adhesion by using T4 mutants lacking pilus components or subpopulations derived from the wild type strain and characterized to be highly (95%) or poorly (5%) piliated. This allowed us to evaluate not only the contribution in adhesion of the single pilus subunits but also to examine the influence of the entire pilus structure by comparing isogenic populations differing only in pilus expression. The data clearly indicated that the single disruption of *rrga* or *rrgb* genes as well as the absence of polymerized pili on the surface of bacteria resulted in

the same level of adherence, suggesting that both the presence of the adhesin and its correct spacing from the bacterial cell were equally important. Some published evidences exist that the RrgA molecule is incorporated into the pilus shaft at the terminal tip of the polymerized structure and that the contemporary deletion of *rrgb* and *rrgc* genes results in its localization on the bacterial cell surface (Nelson et al., 2007; Hilleringmann et al., 2009) were RrgA still retains its adhesive properties on A549 epithelial cells. Our data differs from this analysis as the TIGR4 Δ *rrgb* strain results less adhesive than the wild type strain on almost all the cell lines tested. As the RrgC molecule has been assigned the role of anchoring the polymerized pilus to the bacterial cell wall (Hilleringmann et al., 2009) and thus results irrelevant to compare a double *rrgc/rrgb* and a *rrgb* mutant focusing at the final RrgA localization, this divergence could be explained by the fact that we do not use a centrifugation step during the adhesion assay as this could lead to an aspecific binding of bacteria to the monolayer. In our model, indeed, TIGR4 Δ *rrgb* strain was less adherent if compared to the isogenic wild type strain, supporting the hypothesis that the pilus structure should have the primary function to take the adhesin far from the surface with the opportunity to reach host ligands that are distal from the bacterial cell. Once defined the role in adhesion of TIGR4 pilus and of its constitutive subunits RrgA and RrgB, we tested the pilus mediated adhesiveness of different pneumococcal strains that could be successfully divided into sub-populations highly (H) or poorly (L) expressing pili. By comparing the H sub-populations we noticed a great variability in absolute adhesion values among the strains tested while the low-expressing sub-populations showed the same level of adherence. This finding suggests that in the absence of pili the overall adhesive capacity among the strains tested is almost the same, highlighting the importance of this structure for pneumococcal adhesiveness. Moreover, the fact that T4 pilus-dependent adhesion is extremely higher with respect to the other strains tested suggests that there must be key differences among pilus sub-units of different strains or that may exist cellular determinants that can affect pilus-dependent adhesion capability. Since *S.pneumoniae* is known to produce high amounts of polysaccharide capsule to protect itself from the immune system, we asked if the variability among the pilus expressing sub-populations could depend on the production of the capsule rather than on differences linked to variation of pilus components. Indeed we found that there was an inverse correlation between capsule production and pilus dependent adhesive properties among the strain tested. Furthermore we demonstrated that the deletion of the capsular locus in the poorly adherent strain 19FTaiwan resulted in a considerable increase in the adhesion to epithelial cells, at levels comparable to that of poorly capsulated T4 strain. These results confirmed our hypothesis that the great

adhesion variability among the strains tested relied on a different exposure of pili rather than on sequence differences between the sub-unit pilus components. This finding is in agreement with published results indicating that pathogens actively modulate capsule production with the aim to balance their need to escape from the immune system and the exigency to firmly adhere to the host mucosal tissues (Hammerschmidt et al., 2005). We also aimed at understanding if anti-pilus antibodies other than being functional in killing were capable to reduce pneumococcal adhesiveness to human epithelial cells. Both anti-RrgA and anti RrgB antibodies interfered with adhesion to epithelial cells in a dose dependent manner suggesting that anti-pilus antibodies could reduce pneumococcal adhesiveness during colonization of host niches. Furthermore, a monoclonal antibody against RrgA was able to compete with adhesion in a similar manner with respect to the polyclonal serum against the whole protein. This finding is of extreme importance since it can be argued that the binding of the monoclonal antibody to a single RrgA epitope is sufficient to inhibit the adhesive properties of the molecule. Epitope mapping experiments resulted in the identification of the possible binding region on the RrgA molecule, located in the c-terminal domain, the most variable part of the protein. At the moment we are trying to confirm this result by producing point-mutated forms of RrgA with the scope to select mutants that are not recognized by the functional monoclonal antibody and finally complement rrgA ko strain with these sequences to confirm the importance of the epitope in the adhesion to human epithelial cells.

